

1 **Genetically Engineered Proteins with Two Active Sites for Enhanced Biocatalysis and**
2 **Synergistic Chemo- and Biocatalysis**

3

4 Sandra Alonso^{1,10}, Gerard Santiago^{2,10}, Isabel Cea-Rama^{3,10}, Laura Fernandez-Lopez¹, Cristina
5 Coscolín¹, Jan Modregger⁴, Anna K. Ressmann⁴, Mónica Martínez-Martínez¹, Helena Marrero¹,
6 Rafael Bargiela^{5,6}, Marcos Pita¹, Jose L. Gonzalez-Alfonso¹, Manon L. Briand⁷, David Rojo⁸, Coral
7 Barbas⁸, Francisco J. Plou¹, Peter N. Golyshin^{5,6}, Patrick Shahgaldian⁷, Julia Sanz-Aparicio^{3,11,*}, Víctor
8 Guallar^{2,9,11,*} and Manuel Ferrer^{1,11,*}

9 ¹Institute of Catalysis, Consejo Superior de Investigaciones Científicas (CSIC), 28049 Madrid, Spain.

10 ²Barcelona Supercomputing Center (BSC), 08034 Barcelona, Spain. ³Department of Crystallography
11 & Structural Biology, Institute of Physical Chemistry "Rocasolano", CSIC, 28006 Madrid, Spain.

12 ⁴EUCODIS Bioscience GmbH, 1030 Vienna, Austria. ⁵School of Natural Sciences, Bangor University,
13 LL57 2UW Bangor, UK. ⁶Centre for Environmental Biotechnology, Bangor University, LL57 2UW

14 Bangor, UK. ⁷University of Applied Sciences and Arts Northwestern Switzerland, School of Life
15 Sciences, Institute of Chemistry and Bioanalytics, CH-4132 Muttenz, Switzerland. ⁸Centro de

16 Metabolómica y Bioanálisis (CEMBIO), Facultad de Farmacia, Universidad CEU San Pablo, 28668
17 Boadilla del Monte, Madrid, Spain. ⁹Institució Catalana de Recerca i Estudis Avançats (ICREA),

18 08010 Barcelona, Spain. ¹⁰These authors contributed equally: Sandra Alonso, Gerard Santiago, and

19 Isabel Cea-Rama. ¹¹These authors equally coordinated the work: Julia Sanz-Aparicio, Víctor Guallar
20 and Manuel Ferrer. *e-mail: xjulia@iqfr.csic.es (J.S-A.); victor.guallar@bsc.es (V.G.);

21 mferrer@icp.csic.es (M.F.).

22 **Enzyme engineering has allowed not only de novo creation of active sites catalysing known**
23 **biological reactions with rates close to diffusion limits, but also the generation of abiological sites**
24 **performing new-to-nature reactions. However, catalytic advantages of engineering multiple**
25 **active sites into a single protein scaffold are yet to be established. Here, we report on proteins**
26 **with two active sites of biological and/or abiological origin, for improved natural and non-**
27 **natural catalysis. The approach increased catalytic properties, such as enzyme efficiency,**
28 **substrate scope, stereo-selectivity, and optimal temperature window of an esterase when**
29 **containing two biological sites. Then, one of the active sites was metamorphosed into a metal-**
30 **complex chemocatalytic site for oxidation and Friedel-Crafts alkylation reactions facilitating**
31 **synergistic chemo- and biocatalysis in a single protein. The transformation of 1-naphthyl acetate**
32 **to 1,4-naphthoquinone (conversion *ca.* 100%) and vinyl crotonate/benzene to 3-phenylbutyric**
33 **acid ($\geq 83\%$; e.e. $>99.9\%$) was achieved in one-pot by this artificial multi-functional**
34 **metalloenzyme.**

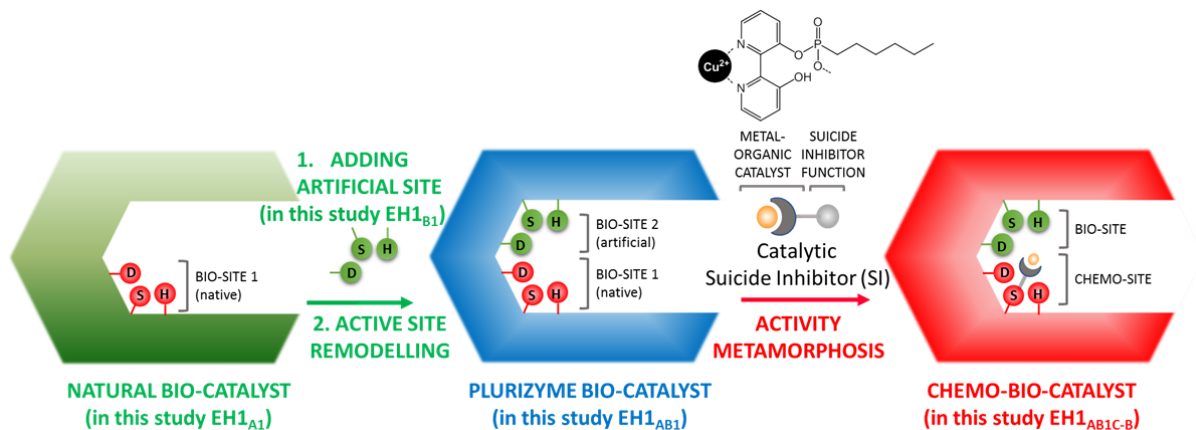
35 The field of enzyme engineering has developed considerably over the last decade, opening great
36 potential for applications ranging from greener production processes and diagnostics to therapeutic
37 usage and biomedicine. Directed evolution and computation-driven rational mutagenesis are fostering
38 such developments¹⁻⁴. These techniques allow optimization of biocatalysts by tuning substrate
39 specificity and improving the activity and/or stability under operational conditions. In addition,
40 significant efforts in *de novo* enzymatic active site design are being undertaken, although directed
41 evolution and protein engineering are required to boost the activity of the original computational
42 design. The introduction of biocatalytic sites into non-catalytic protein scaffolds also opens new
43 opportunities⁵⁻⁹. As such, certain artificial enzymes approach the diffusion limit while still catalysing
44 the desired reaction using a single artificial active site, with turnover rates as high as those of some
45 natural enzymes ($1-5 \text{ s}^{-1}$)¹⁰⁻¹².

46 There are also examples in which catalytically competent organometallic complexes have been
47 introduced in proteins that serve as scaffolds to generate artificial metalloenzymes (ArMs). The first
48 examples of ArMs date back to the late 1970s, when Wilson and Whitesides introduced a diphosphine
49 rhodium (I) biotin derivative into a streptavidin scaffold. The authors demonstrated that this achiral
50 chemocatalyst, located in the asymmetric environment of the biotin-binding site of streptavidin, was
51 capable of chiral hydrogenation of α -acetamido-acrylic acid¹³. However, this work, possibly owing to
52 the unenthusiastic conclusions drawn by the authors, did not attract the attention of the scientific
53 community. It was only the early 2000s that a resurgence of interest in ArMs began, fuelled by
54 advances in both organometallic catalysis and protein engineering¹⁴. Since then, a large number of
55 ArMs, created through the docking of catalytically competent molecules into protein scaffolds by
56 covalent, supramolecular, dative, and metal substitution, have been described. While the catalytic
57 performance of such ArMs, shown to be competent for catalytic reactions including hydrolysis,

58 reduction, oxidation, C-C bond-forming and C-heteroatom bond-forming, has long been inferior to
 59 that of their natural counterparts, recent efforts combining catalyst design and modern protein
 60 engineering allowed bridging of this gap^{14,15}. For example, the Ward group developed a directed
 61 mutation strategy to produce thousands of protein variants and selected the most active one capable of
 62 catalysing metathesis reactions in cells¹⁶. Additionally, the Roelfes group developed artificial copper-
 63 bipyridine catalysts capable of enantioselective Friedel-Crafts alkylation by *in vivo* incorporation, in a
 64 protein scaffold, of metal-binding unnatural amino acids¹⁷ or by the creation of an artificial active site
 65 capable of copper-binding¹⁸.

66 Despite significant efforts directed at introducing single artificial biological⁵⁻¹² or abiological¹³⁻¹⁸
 67 catalytic entities into a protein scaffold, the introduction of multiple active sites, either biological or
 68 non-natural, and the analysis of the catalytic advantages it can have, is rare. The only examples are
 69 protein scaffolds with two heme, Fe-S or copper sites catalysing the same chemistry^{14,18-22}, or a recent
 70 engineered lipase into which a catalytic metal has been introduced²³. Although, this last design can
 71 potentially confer the capacity for cascade reactions, the catalysis was done in a two-step fashion,
 72 changing the reaction conditions, precluding synergistic effects.

73 Here, we report an approach that exploits the possibility to genetically engineer proteins with two
 74 biological active sites, and furthermore, its expansion allowing its further metamorphosis into a
 75 protein with both biological and abiological active sites (Fig. 1). Results are presented demonstrating
 76 the broad potential and versatility of the presented procedure to create biocatalysts with improved
 77 catalytic properties, and metallo-enzymes capable of cascade reactions where an active synergy of
 78 both biological and abiological catalytic entities exists.



79
 80

81 **Fig. 1 General concept for engineering proteins with two active sites.** The concept consists of
 82 the following sequential workflow. First, a target natural enzyme (*e.g.* a serine ester hydrolase in this
 83 study), containing a biological active site (BIO-SITE 1 in figure), is selected. Second, by applying
 84 Protein Energy Landscape Exploration (PELE) software, an extra potential binding pocket to
 85 introduce an artificial biological active site (*e.g.* a nucleophilic serine in this study) is identified, which

can be further remodelled to achieve an optimal configuration (BIO-SITE 2). Third, through the differential affinity for a suicide phosphonate inhibitor bearing a metal-organic complex, one of the biological sites is metamorphosed into a copper-based chemocatalytic (or abiological) site (CHEMO-SITE), while the other site retains its own biological activity.

Results

Design of a protein with two biological active sites and its catalytic advantages

Improving the efficiency of enzymes is rapidly becoming a necessity. One could imagine attacking the problem by engineering more and more reactive sites into a single enzyme scaffold, which by a synergetic effect may improve catalysis. We named this concept as *plurizyme* (the Latin root *pluri*: multiplicity). However, the first trial of introducing a second artificial active site into a serine esterase containing a natural one could not bring in catalytic advantages (Supplementary Note 1)²⁴. Here, through providing a better spatial configuration we designed a new artificial design (EH1_{B1}; Supplementary Figure 1) with boosted catalytic performance, in such a way that its incorporation to the natural enzyme (EH1_{A1}) intensified the k_{cat} (average: *ca.* 3.4-fold; *max.*: *ca.* 74-fold) and k_{cat}/K_m (average: *ca.* 94-fold; *max.*: *ca.* 5000-fold) for ester hydrolysis, increased the stereo-selectivity by *ca.* 1100-fold (e.e. >99.9%), and broadened by *ca.* 20°C the temperature at which the enzyme retained more than 80% of the optimal (Fig. 2). It also expanded the substrate spectra, as the resulting *plurizyme* with the two sites (EH1_{AB1}) has the ability to hydrolyze all substrates (78, in total) that each site, combined, convert (Supplementary Figure 2).

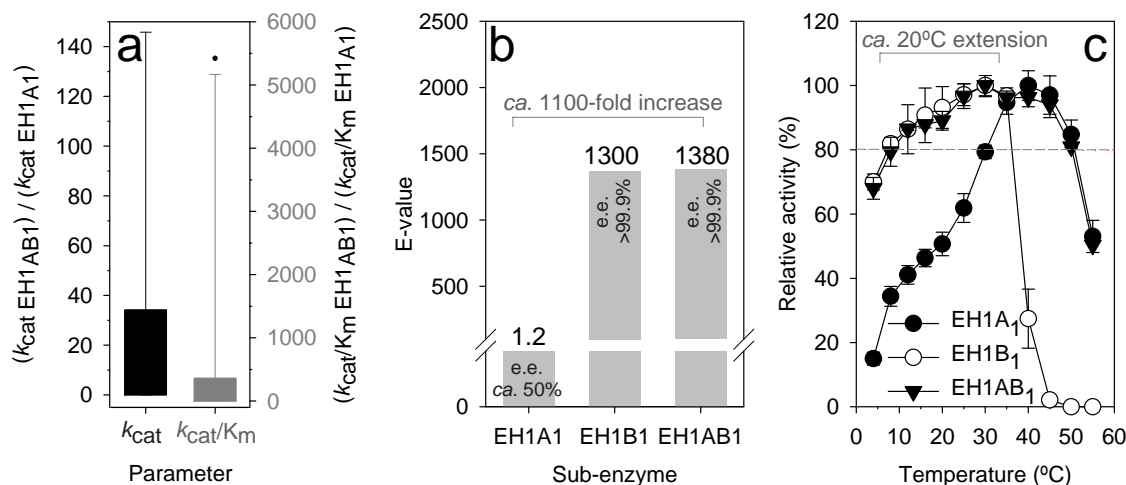


Fig. 2 Bio-catalytic advantages of having two biological active sites. **a**, The artificial site (EH1_{B1}) intensifies the catalytic efficiency. Shown is the bar plot illustrating the relative increase of k_{cat} (left axis) and k_{cat}/K_m (right axis) values of the EH1_{AB1} *plurizyme* with the two sites vs the original EH1_{A1} enzyme with a single active site, for all substrates converted. **b**, The artificial site introduces stereo-specificity. Shown are the average E-values and e.e., determined by gas chromatography, for

112 the kinetic resolution of a racemic mixture of methyl (2*R/S*)-2-phenylpropanoate (*R*-specificity) by the
113 three sub-enzymes. Experimental conditions, raw data and standard deviations for these and other
114 substrates are given in Supplementary Note 2 (Supplementary Figures 2-3, Supplementary Tables 1-
115 2). **c**, The artificial site expands the optimal temperature window. Shown are the temperature profiles
116 of the three sub-enzymes. For T_{opt} determination, calculated on a continuous pH indicator assay²⁴,
117 conditions are as follows - [protein]: 4.5 $\mu\text{g/ml}$; [glyceryl tripropionate]: 50 mM; reaction volume: 44
118 μl ; T: 4-55°C; pH: 8.0. The data, calculated from three independent assays \pm standard deviations
119 (calculated using Excel version 2019) and not fitted to any model, represent the relative percentages
120 (%) of specific activity expressed as U mg^{-1} , compared with the maximum.

121

122 Together, engineering multiple active sites with identical chemistry catalyzed can thus help,
123 through differences in specificity, affinity, turnover rates and local stabilities, intensifying the original
124 bio-catalytic properties of, or conferring new properties (*e.g.* stereo-specificity and expanded working
125 temperature) to, a natural enzyme, herein exemplified by a serine ester-hydrolase. For detailed
126 description of the engineering approach, and detailed experimental and results information see
127 Supplementary Note 2 (Supplementary Figures 2-3, Supplementary Tables 1-2).

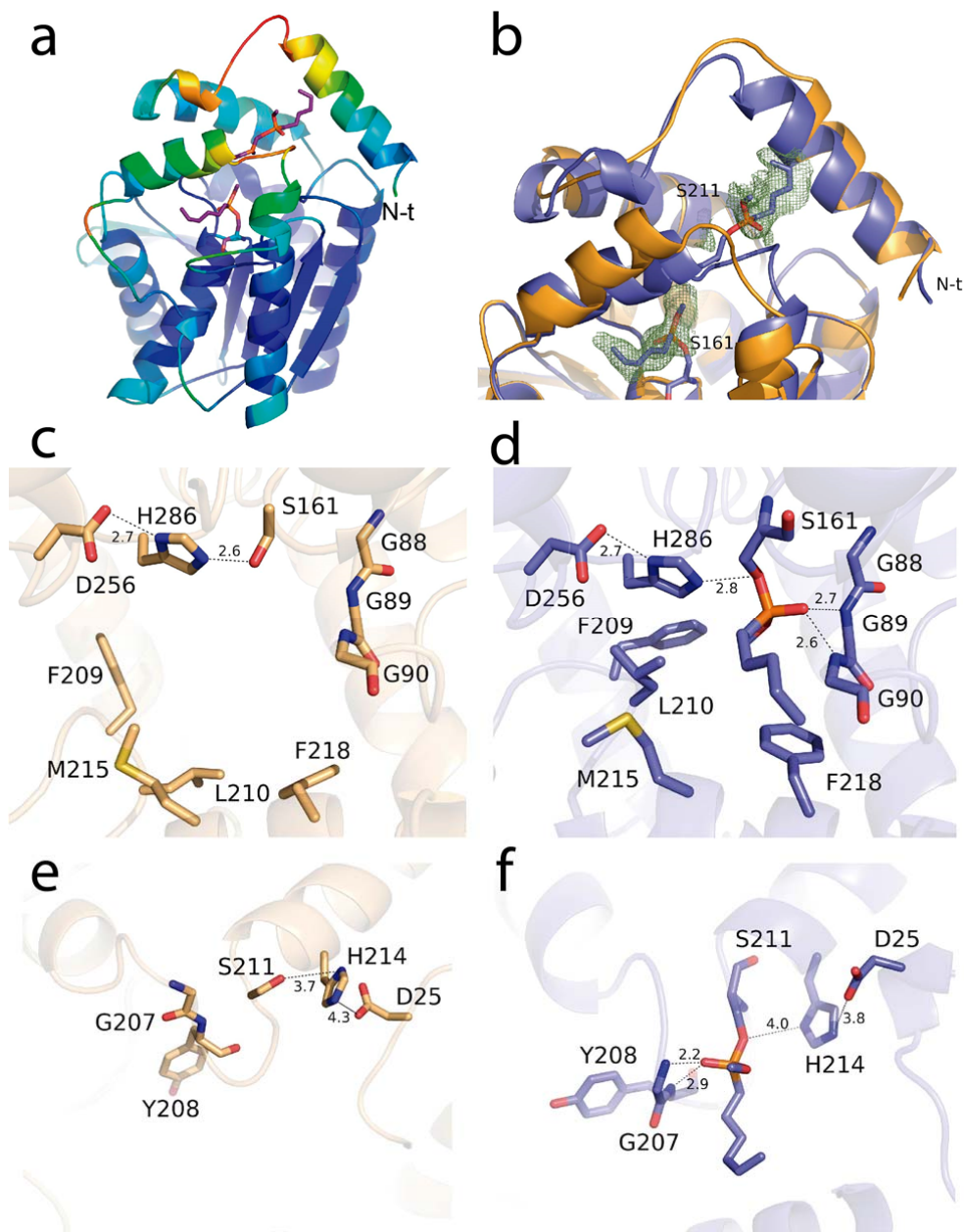
128

129 **Structural evidences of a *plurizyme* with two biological active sites**

130 To prove that both active sites of our *plurizyme* (EH1_{AB1}) are capable of substrate binding and that
131 conversion can occur in both sites, we performed a structural analysis. We obtained crystals from
132 EH1_{AB1} diffracting at 2.1 Å resolution. These crystals were cocrystallized with the suicide inhibitor
133 methyl 4-nitrophenyl hexylphosphonate (M4-4NHP) to obtain the corresponding derivative complex,
134 with two molecules of the inhibitor bound at the catalytic Ser161 (original nucleophile) and Ser211
135 (artificial nucleophile) sites (Fig. 3a; see Supplementary Note 3, Supplementary Figures 4-6). The 4-
136 nitrophenyl phosphonate inhibitor is susceptible to nucleophilic attack by the catalytic Ser, leading to
137 covalent modification and complete inactivation of the enzyme (see Supplementary Note 4,
138 Supplementary Figure 7)^{25,26}.

139 The solved three-dimensional structures show high flexibility in a region (which resembles but
140 does not equal a typical *lid* of lipases) containing the two N-terminal helical regions, Pro4-Gly19 and
141 Ala30-Gly43, which give access to the active-site pocket. Conformational changes are observed at the
142 secondary Ser211 catalytic site, the artificially remodelled site, upon inhibitor binding, as shown in
143 Fig. 3b, which introduce distortions in the packing arrangement within the soaked crystals, explaining
144 the decreased resolution observed (not shown). Nevertheless, the atomic interaction of the inhibitor
145 bound at the two sites can be depicted and is displayed in Fig. 3c-f.

146



147

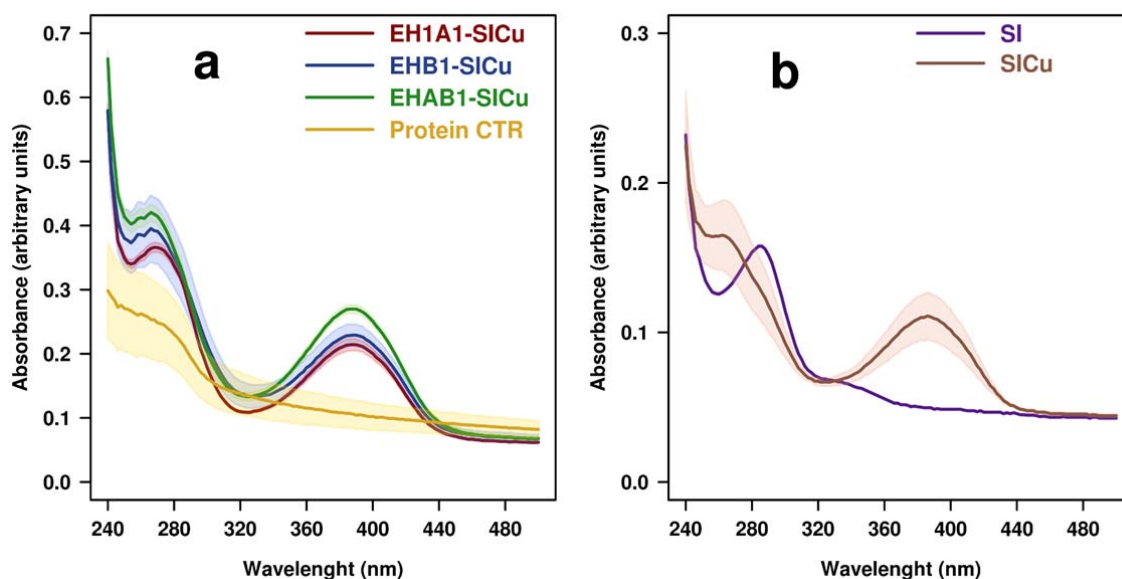
148 **Fig. 3 Crystal structure of EH1_{ABI}.** **a**, Cartoon of the crystallized complex coloured by B factors,
 149 from low (blue) to high (red) with the two bound molecules from the suicide inhibitor M4-4NHP
 150 represented as magenta sticks. **b**, Details of the comparison between the free (orange) and complexed
 151 (slate) EH1_{ABI} showing the conformational changes observed in the environment of Ser211 upon
 152 inhibitor binding. Polder omit maps calculated at the Ser161 and Ser211 catalytic sites displayed at 3.0
 153 σ cut-off. **c-f**, Detail of the Ser161 and Ser 211 binding sites in the free (c, e) and complexed (d, f)
 154 crystals showing relevant distances as dashed lines.

155 **Metamorphosis of a *plurizyme* into a protein with biological and abiological active sites**

156 We further designed an approach to build a protein with both biological and abiological sites
 157 supporting different chemistries. For this purpose, here, we used our EH1_{ABI} *plurizyme* as a platform
 158 and a suicide inhibition strategy. This approach, also called mechanism-based inhibition, occurs when
 159 an enzyme covalently binds a substrate analogue through a reaction similar to that normally catalysed
 160 by the enzyme. This reaction is specific and typically occurs with amino acids involved in a catalytic
 161 reaction, resulting in enzyme activity loss²⁵. In the particular case of ester-hydrolases, esters of
 162 phosphonate are long known to stoichiometrically bind to the serine residue of a catalytic triad²⁶. Here,
 163 a Suicide Inhibitor (SI), 3'-hydroxy-[2,2'-bipyridin]-3-yl methyl hexylphosphonate, equipped with a
 164 transition metal-chelating moiety (*e.g.* a bipyridine ligand) was synthesized and used (see
 165 Supplementary Note 5, Supplementary Scheme 1, Supplementary Figures 8-10). This approach is
 166 expected to confer the inhibitor unit with transition metal-based catalytic function^{17,18,27,28}, which will
 167 be brought into one of the two active sites of a *plurizyme*, while the other remains intact (see Fig. 1).

168 As in the case of M4-4NHP used for cocrystallization, we found that SI binds to the native
 169 (Ser161) and artificial (Ser211) nucleophiles, as the treatment of EH1_{A1}, EH1_{B1} and EH1_{ABI} sub-
 170 enzymes with an excess of SI resulted in inactivation of >99% in less than 10 min (see Supplementary
 171 Note 6, Supplementary Figure 11). To verify the bio-conjugation, the SI-modified sub-enzymes were
 172 incubated for 24 h with an excess of Cu(NO₃)₂, and the resulting Cu²⁺-modified sub-enzymes were
 173 extensively dialyzed to remove the uncoupled inhibitor and copper (see Supplementary Methods).
 174 Further, they were analysed by recording λ_{max} at 386 nm, the redox properties of the Cu²⁺-organic
 175 complex, and the molecular mass by electrospray ionization mass spectrometry (ESI-MS).

176 We first observed the presence of a λ_{max} at 386 nm in all three modified sub-enzymes (Fig. 4a),
 177 which is characteristic of a Cu²⁺-bipyridine complex (Fig. 4b)^{17,18}; this signal was not detected for the
 178 proteins without copper addition (Fig. 4a).

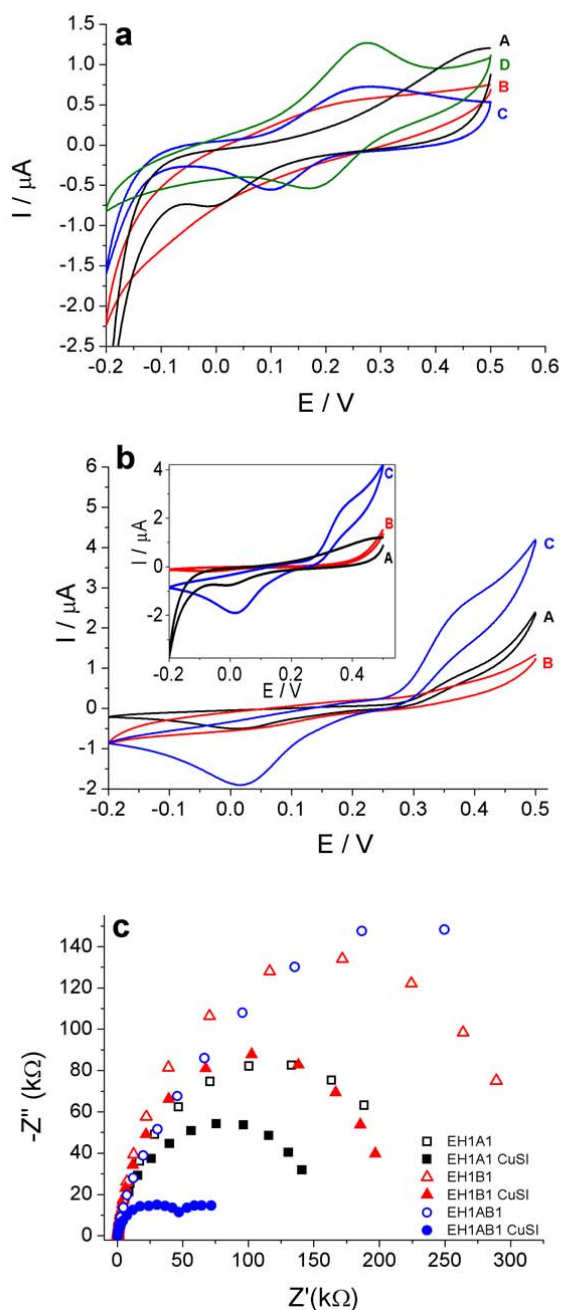


179

180 **Fig. 4 Absorption spectra of modified and un-modified sub-enzymes. a**, Incorporation of Cu^{2+} -SI
181 (SICu) as detected by UV-vis spectroscopy. Spectra were recorded in 96-well plates using Cu^{2+} -
182 modified sub-enzymes (15 μM) prepared with an excess (120 μM) of inhibitor and Cu^{2+} (see
183 Supplementary Methods) in a total volume of 200 μl . Modified sub-enzymes prepared with an excess
184 (120 μM) of inhibitor but without copper salt are shown as a control. **b**, The UV-vis spectra of SI and
185 Cu-modified SI inhibitor (SICu) at 15 μM in a total volume of 200 μl . Shown are average values with
186 a standard deviation of triplicates (calculated using Excel version 2019) shown as shadows; in the case
187 of the control sample, the average value and standard deviation of all three sub-enzymes measured in
188 triplicate are shown.

189
190 By recording the cyclic voltammetry electrochemical response on 3-mercaptopropionic acid
191 (MPA)-modified gold electrodes (Supplementary Note 6, Supplementary Figure 12), we further
192 observed a different behaviour between the free Cu^{2+} -organic complex and the SICu complex, which
193 shows an expected lower electrochemical reversibility due to the chelation of the Cu^{2+} cation in the SI
194 chelating pocket (Supplementary Note 6, Supplementary Figure 13). When SICu was located in the
195 protein scaffold (Fig. 6a) the copper electrochemical signal became more reversible. Results not only
196 showed that the copper complex is effectively inside the corresponding sub-enzymes active sites, but
197 that the electrochemical peaks have shifted and the copper redox signals differs when located in each
198 sub-enzyme (Fig. 6a). Such differences are better spotted in the sub-enzyme with two active sites
199 (EH1_{AB1}) which, due to the presence of two binding Cu^{2+} sites, has an extra increase in the signal of
200 Cu^{2+} compared to sub-enzymes A1 (EH1_{A1}) and B1 (EH1_{B1}) which contains only one. It is also worth
201 pointing out that there is no electrochemical response at the free SICu potentials, suggesting that the
202 inhibitor does not leak out of the binding pocket. The recording of the oxidation of catechol also
203 showed a higher catechol oxidation activity of the EH1_{AB1} -SICu biocatalyst compared EH1_{A1} -CuSI
204 and EH1_{B1} -CuSI (Fig. 6b), not observed in the absence of CuSI (Fig. 6b inset). Catechol did not
205 behave as electrochemical substrate and the process does not fulfil all the requirements to be
206 considered a bioelectrocatalytic oxidation process; however, the enzymes behave as an electron
207 transfer relay that allows the oxidation of catechol at its non-catalytic potential (0.25V vs Ag/AgCl;
208 see Supplementary Note 6). Impedance spectroscopy measurements were also performed using
209 catechol as the redox electrochemical probe. Impedance spectroscopy showed a similar trend for each
210 sub-enzyme: modified sub-enzymes displayed in every case a lower electron transfer resistance than
211 non-modified ones. Nyquist plots allow calculating the charge transfer resistance (R_{ct}) between the
212 electrodes modified with each sub-enzyme and the catechol (Fig. 6c). Remarkably, the EH1_{AB1} -SICu
213 sub-enzyme offered a 10-fold reduction in the R_{ct} when compared to that of EH1_{AB1} in the absence of
214 SICu, a 3-fold reduction in the R_{ct} when compared to that of EH1_{A1} -SICu and a 4-fold reduction in
215 the R_{ct} when compared to that of EH1_{B1} -SICu. These results suggest that the two active sites of the
216 EH1_{AB1} sub-enzymes contain Cu^{2+} -organic complexes which, because their proximity, facilitates

217 intramolecular electron transfer at levels higher than those shown by modified EH1_{A1} and EH1_{B1} sub-
 218 enzymes containing only one site and one complex (Fig. 6c). Control experiments recorded with the
 219 electrodes modified with enzymes lacking CuSI, which yielded no electrochemical response of
 220 catechol, support the need of CuSI-socketed enzymes to allow an electronic path to the electrode
 221 surface. Such electronic path is more likely intramolecular, as there is no sign of CuSI leakage, and an
 222 extramolecular electron path would imply the cooperation of different enzymes, a less likely
 223 mechanism. For detailed description of the electrochemical characterization and electrode and probe
 224 design see Supplementary Note 6 (Supplementary Figures 12-18).



225

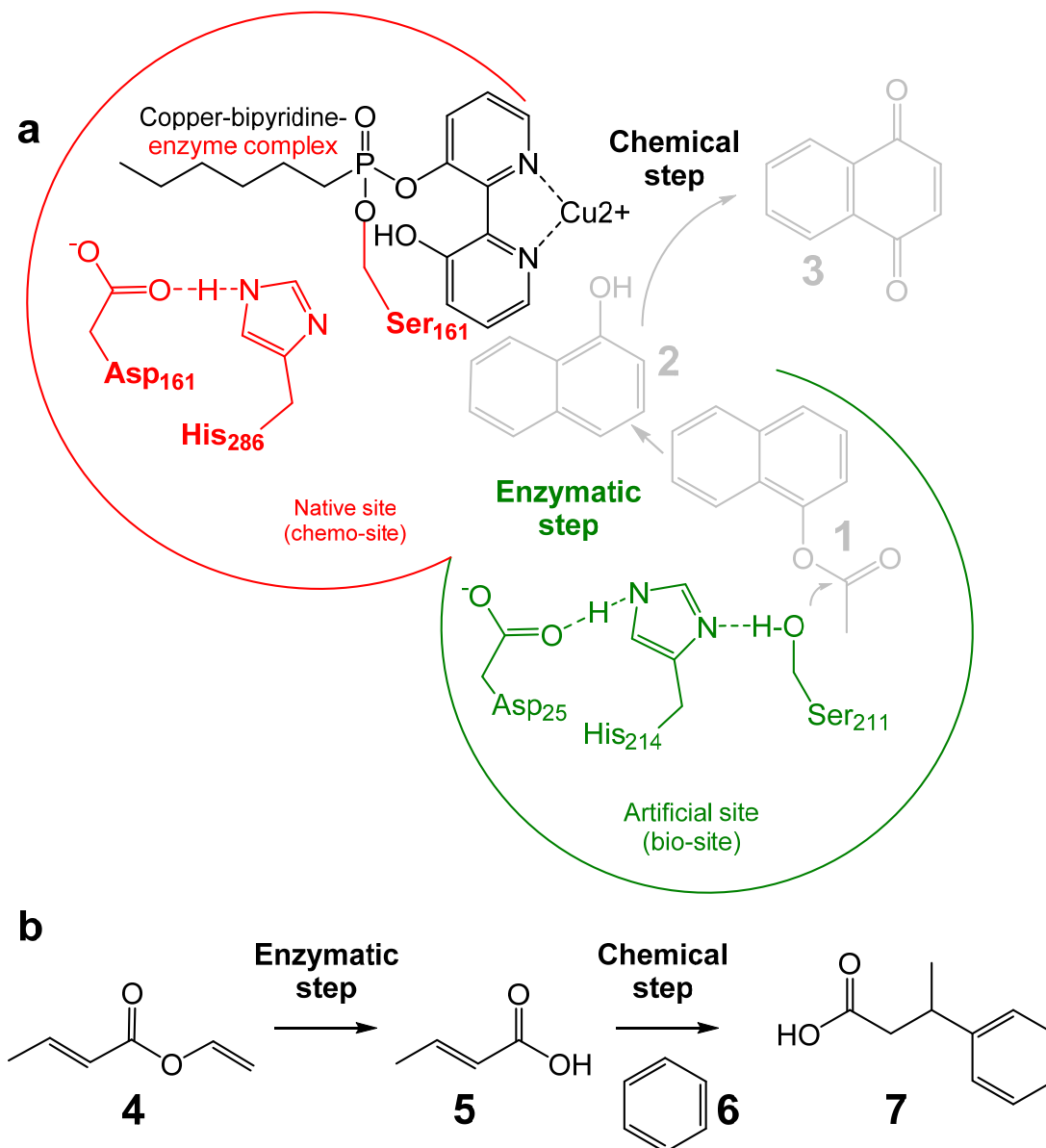
226

227 **Fig. 5 Electrochemical characterization of the chemo-bio catalysts.** **a**, Electrochemical signals of
228 MPA-gold electrodes modified with (A) CuSI, (B) EH1_{A1}-CuSI, (C) EH1_{B1}-CuSI and (D) EH1_{AB1}-
229 CuSI. The CuSI concentration added was *ca.* 0.43 mM. All measurements were recorded using a 20
230 mV·s⁻¹ scan rate and 50 mM phosphate buffer pH 6.5 electrolyte. The working electrode was a gold
231 disk with a 0.2 cm² diameter modified with an MPA SAM. The reference electrode was 3 M Ag/AgCl,
232 and the counter electrode was Pt wire. **b**, Oxidation of catechol (1 mM) by MPA-gold electrodes
233 modified with (A) EH1_{A1}-CuSI, (B) EH1_{B1}-CuSI and (C) EH1_{AB1}-CuSI (process from 0.3 to 0.5 V).
234 Inset: electrochemical responses to catechol measured with MPA-gold electrodes modified with (A)
235 CuSI, (B) EH1_{AB1} in absence of CuSI and (C) EH1_{AB1} in presence of CuSI. **c**, Impedance spectroscopy
236 showing that EH1_{AB1}-CuSI presents a much lower electron transfer resistance than any other
237 combination of sub-enzymes with or without CuSI. Impedance measurements were performed using
238 catechol 1 mM, a bias potential of 0.35 V vs Ag/AgCl. The experimental setup (sub-enzyme
239 concentration *ca.* 0.43 mM) was the same 3-electrode configuration used for cyclic voltammetry.
240

241 Together, results confirm that the SI herein synthesized can be used as a platform to introduce a
242 Cu²⁺-organic complex into our genetically engineered *plurizyme* through the elimination of the
243 methoxy group of the suicide inhibitor and the coupling of a 3'-hydroxy-[2,2'-bipyridin]-3-yl moiety
244 capable of copper binding. The bio-conjugation of two organic complexes to EH1_{AB1} and one to
245 EH1_{A1} and EH1_{B1} was also confirmed by ESI-MS (Supplementary Note 6, Supplementary Figure 19).

246 The fact that, under excess conditions, the conjugation occurs at both active sites might be a
247 disadvantage, as our primary objective was to create a *plurizyme* variant, hereafter referred to as
248 EH1_{AB1} chemo-biocatalyst (EH1_{AB1C-B}), in which one of the active sites is replaced by a Cu²⁺-catalyst
249 and the other remains unaltered. To remedy this shortcoming, we evaluated the possibility that both
250 sites have different affinities for the inhibitor; the different affinities for multiple other substrates (see
251 Supplementary Note 2, Supplementary Figure 2) and the differences in catalytic environments of each
252 active site (Fig. 3) indicated such a possible differentiation. This hypothesis was evaluated by
253 measuring the loss of hydrolytic activity of each sub-enzyme (EH1_{A1}, EH1_{B1} and EH1_{AB1}) in the
254 presence of different concentrations of the inhibitor. As shown in Supplementary Note 7 (see
255 Supplementary Figure 20), whereas the native site could be inhibited at very low concentrations (*ca.* 5
256 μM), the artificial one was only inhibited at concentrations above 35 μM. On the basis of the
257 differential active-site affinity, a dose-dependent inhibition strategy was designed that allowed the
258 specific bio-conjugation of the Cu²⁺-organic complex to Ser161 but not to Ser 211 (see Supplementary
259 Methods; Supplementary Note 7, Supplementary Figure 21). As such, an EH1_{AB1} variant in which the
260 Cu²⁺-organic complex was bio-conjugated at the native active site but not the artificial site could be
261 obtained (Fig. 6), with a coupling efficiency and purity higher than 98% (see Supplementary Note 7,

262 Supplementary Figures 22-23). This result was confirmed by applying this strategy to each of the sub-
 263 enzymes and by confirming the increase in mass by ESI-MS and the λ_{max} at 386 nm by UV/vis
 264 absorption spectroscopy (see Supplementary Note 7, Supplementary Figures 22-24). As an additional
 265 experimental confirmation, we cocrystallized EH1_{ABI} with the CuSI complex (see Supplementary Note
 266 3, Supplementary Figure 6). Despite its moderate resolution (2.79 Å), the electron density confirmed
 267 binding of the ligand only to the native active site. However, the poor quality at the copper-bipyridine
 268 moiety impeded modelling of this portion, which might be attributed to disorder or partial occupancy.
 269



270
 271
 272
 273

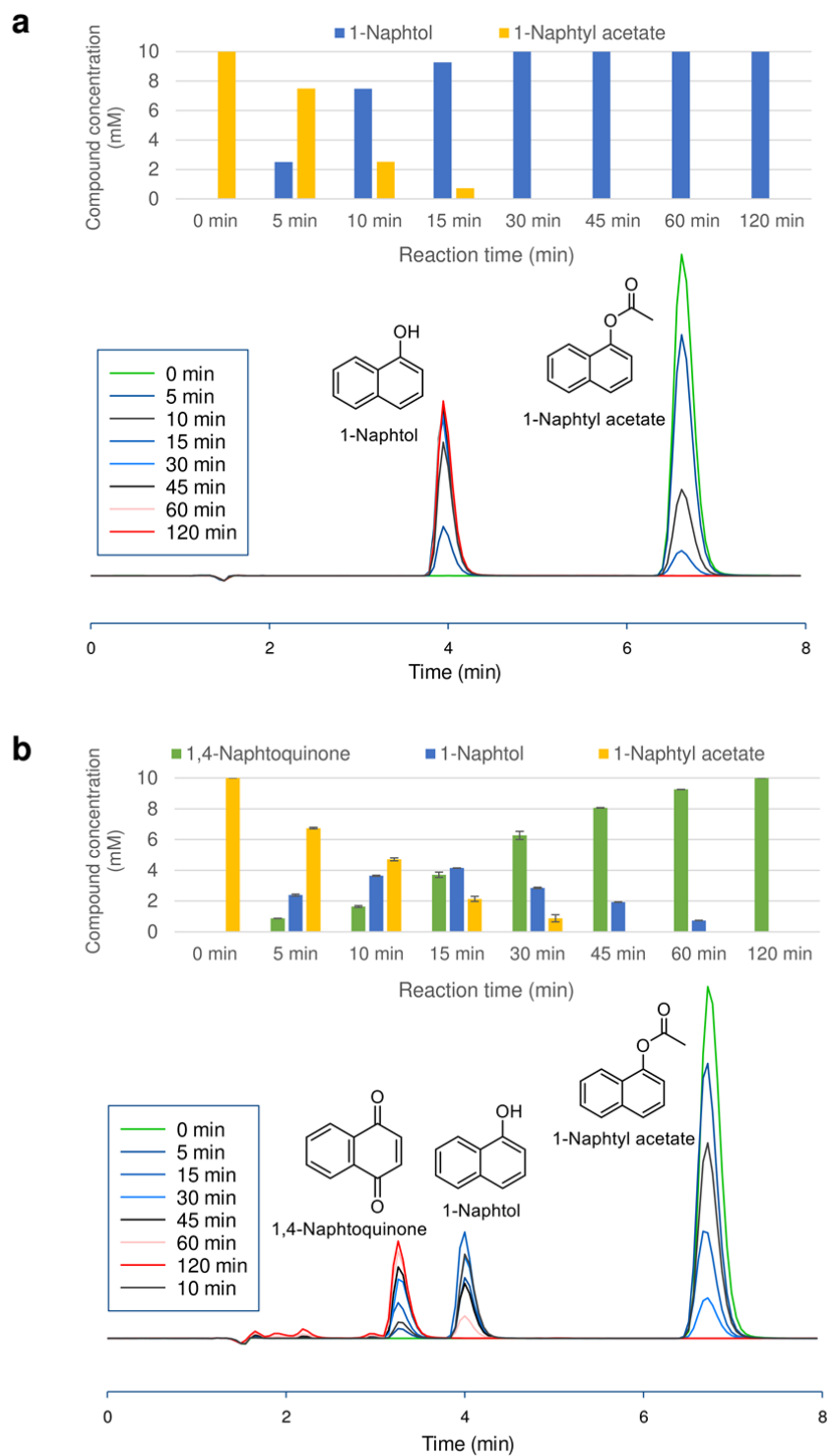
Fig. 6 Image representing the chemo-biocatalyst EH1_{ABI-C-B} generated in this study and its utilization in two model reactions. **a**, Schematic representation of the EH1_{ABI-C-B} design. Colour code

274 as follows: green, the artificial enzymatic site; red: the native site; black: copper-bipyridine molecule
275 placed in the native site. In grey colour, the one-pot conversion of 1-naphthyl acetate (**1**) to naphthol
276 (**2**) by the enzymatic site and its further oxidation to 1,4-naphthoquinone (**3**) by the metal-complex site
277 are illustrated. **b**, Model one-pot conversion of vinyl crotonate (**4**) to crotonic acid (**5**) by the
278 enzymatic site, and its further Friedel-Crafts alkylation to β -phenylbutyric acid (**7**) by the metal-
279 complex site in the presence of benzene (**6**).
280

281 **Synergistic catalysis of the biological with the abiological active site**

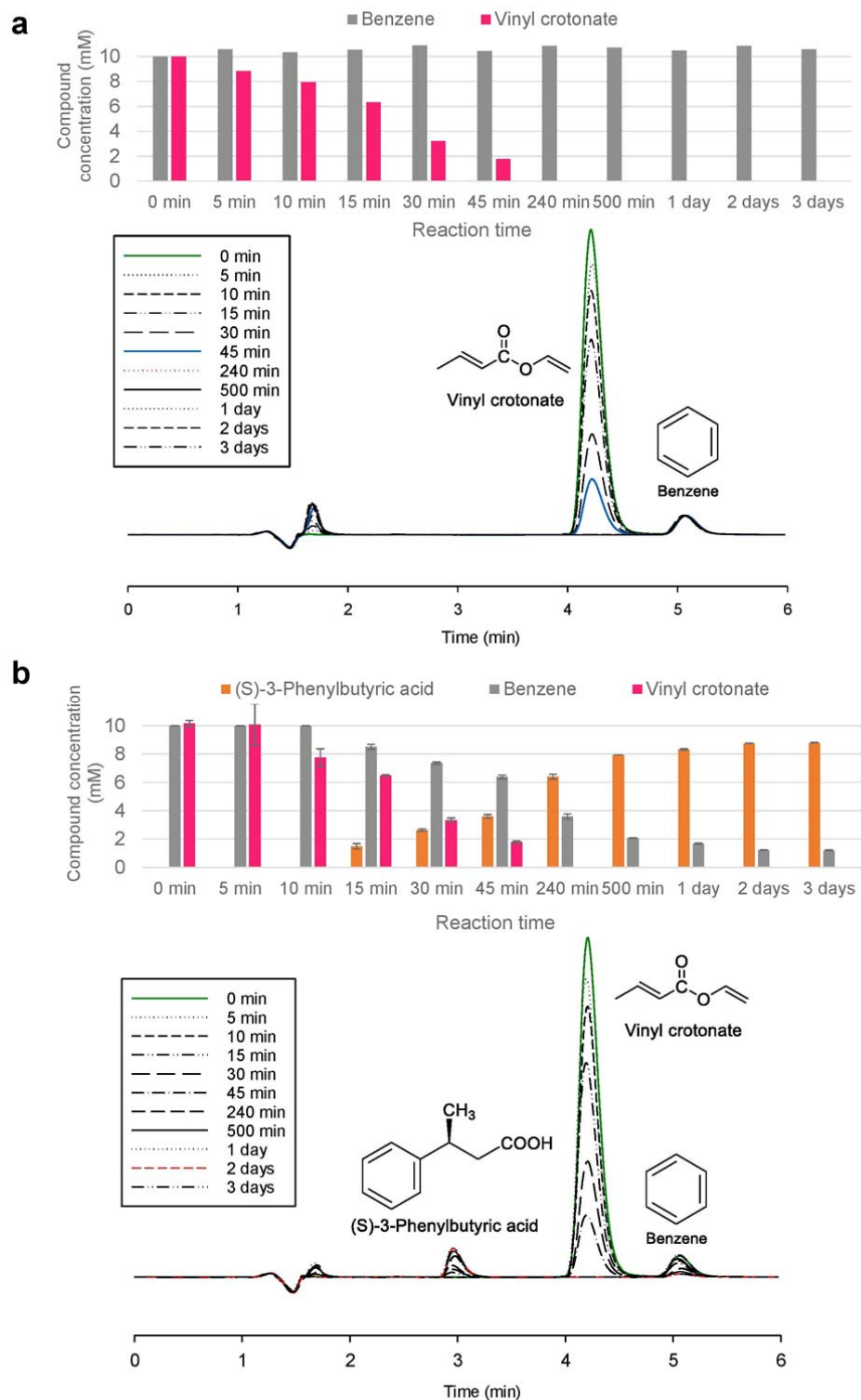
282 The catalytic activity of EH1_{ABIC-B} (Fig. 6a) was evaluated in 2 cascade reactions, which consist of the
283 enzymatic hydrolysis of an ester, followed by a copper-bipyridine oxidation (Fig. 6a, in grey colour)
284 or a Friedel-Crafts alkylation reaction (Fig. 6b). In the first target reaction, enzymatic hydrolysis of
285 ester **1** will produce alcohol **2**, which may be oxidized by the copper-bipyridine catalyst to quinone **3**.
286 This reaction was selected based on the fact that electrochemical tests demonstrated an electron
287 transfer capacity by copper-bipyridine. Ester **1** was selected because it is a polyphenol ester for which
288 the artificial esterase site shows a high conversion rate (see Supplementary Note 2, Supplementary
289 Figure 2, Supplementary Table 1). In the second target reaction, enzymatic hydrolysis of ester **4** will
290 produce the alkenyl fatty acid **5**, which in the presence of benzene (**6**) may yield β -phenylbutyric acid
291 (**7**)⁴⁰. This model reaction was selected because copper-bipyridine catalysts have been shown to
292 perform vinylogous Friedel-Crafts alkylation reactions^{17,18}; ester **4** was selected because it was well
293 converted by the artificial site (see Supplementary Note 2, Supplementary Figure 2, Supplementary
294 Table 1), and the resulting hydrolysis product can be coupled with benzene.

295 The first reaction (Fig. 6a) was carried out at pH 8.0 and 25°C using 10 mM ester **1**. Using a
296 modified protein not containing Cu²⁺, no quinone **3** was formed, but formation of alcohol **2** (100%
297 conversion) was found (Fig. 7a). This result was expected because the only active site was the
298 biocatalytic site. However, in the presence of the chemo-biocatalyst, the conversion to quinone **3**
299 reached 100% after a 2 h reaction (Fig. 7b). The second reaction (Fig. 6b) was carried out at 4°C for 3
300 days following conditions described elsewhere^{17,18}. Using a modified protein not containing Cu²⁺, only
301 crotonic acid (**5**) was formed, and benzene (**6**) remained without consumption (Fig. 8a), whereas in the
302 presence of the chemo-biocatalyst, the conversion reached 83% for product **7** after 3 days (Fig. 8b).
303 The high activity level of the artificial ester-hydrolase active site (Fig. 2c; see Supplementary Note 2,
304 Supplementary Figure 3) at 4°C helps achieve a high conversion rate for the enzymatic step and the
305 concomitant production of product **7**. Interestingly, the product was obtained with a 99% e.e. for (*S*)-3-
306 phenylbutyric acid (see Supplementary Methods). Reaction mixtures obtained in all cases were
307 analysed by ESI-MS (see Supplementary Methods), and the existence of the reaction products was
308 confirmed in each case. We would like to mention that the reaction conditions were not optimized.



309

310 **Fig. 7 One-pot synthesis of 1,4-napthoquinone from 1-napthyl acetate catalysed by EH1_{ABIC-B}.**
 311 **B. a,** Control reaction performed with modified sub-enzyme not containing Cu²⁺. **b,** Reaction in the
 312 presence of EH1_{ABIC-B} containing Cu²⁺. Reaction conditions as follows: - [1-napthyl acetate]: 10 mM;
 313 [sub-enzyme]: 80 μM; T: 25°C; pH: 7.0. Reactions were performed in triplicates with average value
 314 and standard deviations (calculated using Excel version 2019) indicated.



315

316

Fig. 8 One-pot synthesis of 3-phenylbutyric acid from vinyl crotonate and benzene catalysed

317

by EHI_{ABIC-B}. a, Control reaction performed with modified sub-enzyme not containing Cu²⁺. b,

318

Reaction in the presence of EHI_{ABIC-B} containing Cu²⁺. Reaction conditions as follows: - [vinyl

319 crotonate]: 10 mM; [benzene]: 10 mM; [sub-enzyme]: 80 μ M; T: 4°C; pH: 7.0. Crotonic acid
320 (intermediate reaction product) is not detected under our analytical method and is not shown.
321 Reactions were performed in triplicates with average value and standard deviations (calculated using
322 Excel version 2019) indicated.
323

324 The above two examples demonstrated that a protein scaffold with both biological and abiological
325 sites is capable of performing hydrolytic-oxidative and hydrolytic-alkylation one-pot reactions with
326 excellent conversion and enantio-selectivity. From a catalytic point of view, the approach for creating
327 such hybrid catalysts opens novel opportunities compared to previous designs of bio-inspired chemo-
328 catalysts, in which the protein scaffold is mostly a container of a transition metal-complex whose
329 properties are influenced by the microenvironment where it is positioned within the protein scaffold¹⁸.
330 Here, the enzyme also contributes to the catalytic activity. Also, compared to the recent design of a
331 lipase with a Cu^{2+} catalyst²³, where the synergy is not direct and requires, after a first hydrolytic step
332 mediated by the lipase activity, a second reduction reaction just requiring Cu^{2+} and NaBH_4 added to a
333 concentration (*ca.* 15 mg/ml) which may compromise protein integrity and catalyst reutilization⁴¹;
334 thus, in the second reaction the protein does not play an active catalytic role except to immobilize the
335 Cu^{2+} catalyst. In contrast, in our design the reaction is done in one step allowing synergetic catalysis
336 and easy handling; also the cascade reaction produce products in high e.e. that cannot be achieved by
337 the metal cofactor without the protein scaffold.

338 From a methodological point of view, the strategy designed herein to introduce transition metal-
339 complexes can complement the ones previously described, including the metal-binding utilizing
340 cysteine conjugation^{18,23} or unnatural amino acids¹⁷. It is worth mentioning the following advantages.
341 First, our strategy, requiring only side chain replacement, is expected to be versatile in that it can
342 potentially be applied to a large range of enzymes. Second, through the application of PELE
343 simulations, we ensure that the metal-catalyst is located in an area capable of substrate binding⁴².
344 Third, the metal-catalyst is incorporated through a well established suicide inhibition mechanism only
345 requiring the presence of a nucleophilic serine. While introducing two nucleophilic serine may create
346 selectivity problems that do not exist for other bio-conjugation approaches^{18,23}, it is also true that both
347 may have different affinities by which one can control the coupling specificity, as it was shown in the
348 *plurizyme* herein designed. It is also plausible that both sites may have different specificity for other
349 metal-complexes allowing specific bio-conjugation, yet to be investigated, or that in other *plurizymes*
350 to be developed such selectivity problems may not occur because different active site configurations.
351 For additional remarks see Supplementary Note 7.

352

353 **Conclusions**

354 Recent progress in (bio)chemical sciences has enabled the design and production of protein scaffolds
355 artificially endowed with either biocatalytic or chemocatalytic activities. While this is plausible when

356 a single artificial catalytic entity is introduced into a protein scaffold, it is however challenging to
357 introduce multiple sites and activities, including natural and non-natural ones. To what extent can
358 additional sites and activities, either biological and/or abiological, intensify the catalytic performance
359 of protein scaffolds? Overcoming this challenge and finding answers to this question would allow the
360 design of more efficient biocatalysts with improved natural activities and multi-catalytic systems for
361 performing non-natural concerted cascade reactions.

362 Here, an approach to design catalytically active proteins equipped with two enzymatic active sites
363 or an enzymatic and a chemocatalytic site is described, and consists of the following sequential
364 workflow: production of a genetically engineered *plurizyme* with two distinct active sites (e.g. two
365 sites supporting ester hydrolysis in this study) through structure-based modelling – chemical design of
366 a synthetic catalytic suicide inhibitor capable of coordinating a transition metal ion – metamorphosis
367 of one of the serine hydrolytic biological sites into a versatile metal-complex chemocatalytic site
368 through suicide inhibition. We hypothesized this approach may provide technical advantages,
369 including expansion of the diversity of artificial catalysts, and new catalytic opportunities. This was
370 showed by a first example demonstrating that the catalytic properties of a natural serine hydrolase can
371 be significantly boosted by adding an artificial site with an appropriate catalytic configuration, because
372 the additive effect of the two biological (natural and artificial) sites. Results provided in
373 Supplementary Note 8 (Supplementary Figures 25-28, Supplementary Table 3) further demonstrated
374 that the *plurizyme* approach and the catalytic enhancement associated to the introduction of multiple
375 biological sites is reproducible and can be easily extended to other serine ester-hydrolase. A second
376 example is also exemplified by the design of hybrid homogeneous catalysts integrating multi-catalytic
377 units in one, which are capable of performing chemical and biological catalysis in synergy (e.g.,
378 sequential reactions) with excellent conversion and enantio-selectivity. Results provided in
379 Supplementary Note 9 (Supplementary Figures 29-31, Supplementary Table 4) further demonstrated
380 that our design offers advantages compared to traditional multi-catalyst systems²³, as the co-
381 localization of both biological and abiological catalytic entities in a single scaffold was shown to
382 favour substrate and product transfer of one to another and to expand the performance under
383 conditions at which the native catalysts are sub-optimal.

384

385 **Methods**

386 A full description of the methods is available in the Supplementary Information (see Supplementary
387 Methods, and Supplementary Note 10, Supplementary Figures 32-36).

388

389 **Data availability:** The atomic coordinates have been deposited in the Protein Data Bank under
390 accession numbers 6I8F, 6RB0 and 6RKY. All other data is available from the authors upon
391 reasonable request.

392

393 **References**

- 394 1. Bren, K. L. Engineered biomolecular catalysts. *J. Am. Chem. Soc.* **139**, 14331-14334 (2017).
- 395 2. Ebert, M. C. & Pelletier, J. N. Computational tools for enzyme improvement: why everyone
396 can - and should - use them. *Curr. Opin. Chem. Biol.* **37**, 89-96 (2017).
- 397 3. Arnold, F. H. Directed evolution: Bringing new chemistry to life. *Angew Chem. Int. Ed. Engl.*
398 **57**, 4143-4148 (2018).
- 399 4. Acebes, S. et al. Rational enzyme engineering through biophysical and biochemical modeling.
400 *ACS Catal.* **6**, 1624-1629 (2016).
- 401 5. Seelig, B. & Szostak, J. W. Selection and evolution of enzymes from a partially randomized
402 non-catalytic scaffold. *Nature* **448**, 828-831 (2007).
- 403 6. Jiang, L. et al. De novo computational design of retro-aldol enzymes. *Science* **319**, 1387-1391
404 (2008).
- 405 7. Richter, F. et al. Computational design of catalytic dyads and oxyanion holes for ester
406 hydrolysis. *J. Am. Chem. Soc.* **134**, 16197-16206 (2012).
- 407 8. Rufo, C. M. et al. Short peptides self-assemble to produce catalytic amyloids. *Nat. Chem.* **6**,
408 303-309 (2014).
- 409 9. Moroz, Y. S. et al. New tricks for old proteins: single mutations in a nonenzymatic protein give
410 rise to various enzymatic activities. *J. Am. Chem. Soc.* **137**, 14905-14911 (2015).
- 411 10. Blomberg, R. et al. Precision is essential for efficient catalysis in an evolved Kemp eliminase.
412 *Nature* **503**, 418-421 (2013).
- 413 11. Khersonsky, O. et al. Optimization of the in-silico-designed Kemp eliminase KE70 by
414 computational design and directed evolution. *J. Mol. Biol.* **407**, 391-412 (2011).
- 415 12. Röthlisberger, D. et al. Kemp elimination catalysts by computational enzyme design. *Nature*
416 **453**, 190-195 (2008).
- 417 13. Wilson, M. E. & Whitesides, G. M. Conversion of a protein to a homogeneous asymmetric
418 hydrogenation catalyst by site-specific modification with a diphosphinerhodium(I) moiety. *J.*
419 *Am. Chem. Soc.* **100**, 306-307 (1978).
- 420 14. Dydio, P. et al. An artificial metalloenzyme with the kinetics of native enzymes. *Science*, **354**,
421 102-106 (2016).
- 422 15. Lewis, J. C. Artificial metalloenzymes and metallopeptide catalysts for organic synthesis. *ACS*
423 *Catal.* **3**, 2954-2975 (2013).
- 424 16. Jeschek, M. et al. Directed evolution of artificial metalloenzymes for in vivo metathesis. *Nature*
425 **537**, 661-665 (2013).
- 426 17. Drienovská, I. et al. Novel artificial metalloenzymes by *in vivo* incorporation of metal-binding
427 unnatural amino acids. *Chem Sci.* **6**, 770-776 (2015).
- 428 18. Bos, J. et al. Enantioselective artificial metalloenzymes by creation of a novel active site at the
429 protein dimer interface. *Angew. Chem. Int. Ed. Engl.* **51**, 7472-7475 (2012).

- 430 19. Lin, Y.-W. et al. Rational design of heterodimeric protein using domain swapping for
431 myoglobin. *Angew. Chem. Int. Ed.* **54**, 511– 515 (2015).
- 432 20. Farid, T. A. Elementary tetrahelical protein design for diverse oxidoreductase functions. *Nat.*
433 *Chem. Biol.* **9**, 826-833 (2013).
- 434 21. Roy, A. et al. De novo design of an artificial bis[4Fe-4S] binding protein. *Biochemistry* 2013,
435 **52**, 7586-7594 (2013).
- 436 22. Tebo, A. G. & Pecoraro, V. L. Artificial metalloenzymes derived from three-helix bundles.
437 *Curr. Opin. Chem. Biol.* **25**, 65-70 (2015).
- 438 23. Felice, M. et al. Synthesis of a heterogeneous artificial metallolipase with chimeric catalytic
439 activity. *Chem. Commun. (Camb)* **51**, 9324-9327 (2015).
- 440 24. Santiago, G. et al. Rational engineering of multiple active sites in an ester hydrolase.
441 *Biochemistry* **57**, 2245-2255 (2018).
- 442 25. Zollner H. *Handbook of enzyme inhibitors* (Wiley-VCH Verlag GmbH, 1999).
- 443 26. Myers, D. K. Competition of the aliesterase in rat serum with the pseudo cholinesterase for
444 diisopropyl fluorophosphonate. *Science* **115**, 568-570 (1952).
- 445 27. Beller M., Renken A. & van Santen R. A. *Catalysis: from principles to applications* (Wiley-
446 VCH Verlag GmbH, 2012).
- 447 28. Schwizer, F. et al. Artificial metalloenzymes: reaction scope and optimization strategies. *Chem.*
448 *Rev.* **118**, 142-231 (2018).
- 449 29. Wang, T. et al. Rational redesign of the active site of selenosubtilisin with strongly enhanced
450 glutathione peroxidase activity. *J. Catal.* **359**, 27-35 (2018).
- 451 30. Hoque, M. A. et al. Stepwise loop insertion strategy for active site remodeling to generate novel
452 enzyme functions. *ACS Chem. Biol.* **12**, 1188-1193 (2017).
- 453 31. Payer, S. E. et al. A rational active-site redesign converts a decarboxylase into a C=C hydratase:
454 "Tethered Acetate" supports enantioselective hydration of 4-hydroxystyrenes. *ACS Catal.* **8**,
455 2438-2442 (2018).
- 456 32. Zastrow, M. L. & Pecoraro, V. L. Influence of active site location on catalytic activity in de
457 novo-designed zinc metalloenzymes. *J. Am. Chem. Soc.* **135**, 5895-5903 (2013).
- 458 33. Ross, M. R. et al. Histidine orientation modulates the structure and dynamics of a de novo
459 metalloenzyme active site. *J. Am. Chem. Soc.* **137**, 10164-10176 (2015).
- 460 34. Der, B. S., Edwards, D. R. & Kuhlman, B. Catalysis by a de novo zinc-mediated protein
461 interface: implications for natural enzyme evolution and rational enzyme engineering.
462 *Biochemistry* **51**, 3933-3940 (2012).
- 463 35. Khare, S. D. et al. Computational redesign of a mononuclear zinc metalloenzyme for
464 organophosphate hydrolysis. *Nat. Chem. Biol.* **8**, 294-300 (2012).
- 465 36. Zastrow, M. L. et al. Hydrolytic catalysis and structural stabilization in a designed
466 metalloprotein. *Nat. Chem.* **4**, 118-123 (2012).

- 467 37. Dydio, P. et al. An artificial metalloenzyme with the kinetics of native enzymes. *Science* **354**,
468 102-106 (2016).
- 469 38. Zandonella, G. et al. Interactions of fluorescent triacylglycerol analogs covalently bound to the
470 active site of a lipase from *Rhizopus oryzae*. *Eur. J. Biochem.* **262**, 63-69 (1999).
- 471 39. Tokuriki, N. et al. Diminishing returns and tradeoffs constrain the laboratory optimization of an
472 enzyme. *Nat. Commun.* **3**, 1257 (2012).
- 473 40. Koelsch C. F., Hochmann H., Le Claire C. D. The Friedel-Crafts reaction with cinnamic,
474 crotonic, and β -chlorocrotonic acids. *J. Am. Chem. Soc.* **65**, 59-60 (1943).
- 475 41. Blanco R. M. & Guisán J. M. Stabilization of enzymes by multipoint covalent attachment to
476 agarose-aldehyde gels. Borohydride reduction of trypsin-agarose derivatives. *Enzyme Microb.*
477 *Technol.* **11**, 360-366 (1989).
- 478 42. Lecina D., Gilabert J. F. & Guallar V. Adaptive simulations, towards interactive protein-ligand
479 modeling. *Sci Rep.* **7**, 8466 (2017).

480

481 **Acknowledgements**

482 This work was funded by grant ‘INMARE’ from the European Union’s Horizon 2020 (grant
483 agreement no. 634486), grants PCIN-2017-078 (within the Marine Biotechnology ERA-NET),
484 CTQ2016-79138-R, BIO2016-76601-C3-1-R, BIO2016-76601-C3-3-R, BIO2017-85522-R, RTI2018-
485 095166-B-I00, and RTI2018-095090-B-100 from the Ministerio de Economía y Competitividad,
486 Ministerio de Ciencia, Innovación y Universidades (MCIU), Agencia Estatal de Investigación (AEI),
487 Fondo Europeo de Desarrollo Regional (FEDER) and European Union (EU). P.N.G. and R.B.
488 acknowledge the support of the UK Biotechnology and Biological Sciences Research Council
489 (BBSRC; grant No. BB/M029085/1) and the Centre of Environmental Biotechnology Project and the
490 Supercomputing Wales project, which are partly funded by the European Regional Development Fund
491 (ERDF) via the Welsh Government. The authors gratefully acknowledge financial support provided by
492 the ERDF. C. Coscolín thanks the Ministerio de Economía y Competitividad and FEDER for a PhD
493 fellowship (Grant BES-2015-073829). Jose L. Gonzalez-Alfonso thanks the support of Spanish
494 Ministry of Education, Culture and Sport through the National Program FPU (FPU17/00044). I. Cea-
495 Rama thanks the Regional Government of Madrid for a fellowship (PEJ_BIO_AI_1201). Authors
496 would like to acknowledge Sergio Ciordia and María C. Mena for MALDI-TOF/TOF analysis. We
497 thank the staff of the European Synchrotron Radiation Facility (ESRF), Grenoble, France, for
498 providing access and for technical assistance at beamline ID30A-1/MASSIF-1 and the Synchrotron
499 Radiation Source at Alba (Barcelona, Spain) for assistance at BL13-XALOC beamline. Authors would
500 like to acknowledge also to María J. Vicente and Maite A. Pascual at the Servicio Interdepartamental
501 de Investigación (SIDI) from the Autonomous University of Madrid for the ESI-MS analyses.

502

503 **Author contributions**

504 SA, GS and IC-R contributed equally to this work. The manuscript was written through contributions
505 of M. Ferrer, V. Guallar, J. Sanz-Aparicio and P. Shahgaldian. All authors have given approval to the
506 final version of the manuscript. SA, CC, LF-L, MM-M, HM and PNG contributed to site-directed
507 mutagenesis and protein expression, purification and characterization. JM and AKR coordinated, in
508 collaboration with MF, the synthesis of suicide inhibitor. RB contributed to the biochemical data
509 analysis. DR and CB contributed GC analysis for enantioselectivity determination. JLG-A and FJP
510 performed HPLC analysis of the reaction products. GG and VG conducted the PELE simulations and
511 molecular dynamics. MP contributed together with SA and LF-L to the electrochemical measurement.
512 IC-R and JS-A performed the crystallization and X-ray structure determination. MB contributed to
513 protocol development for the inhibition procedure. MF and VG conceived the *plurizyme* work, and
514 MF and PS conceived the metamorphosis of the enzymatic to chemical catalyst. MF wrote the initial
515 draft of the manuscript, which was further written through contributions of VG, JS-A and PS.

516 **Competing interests**

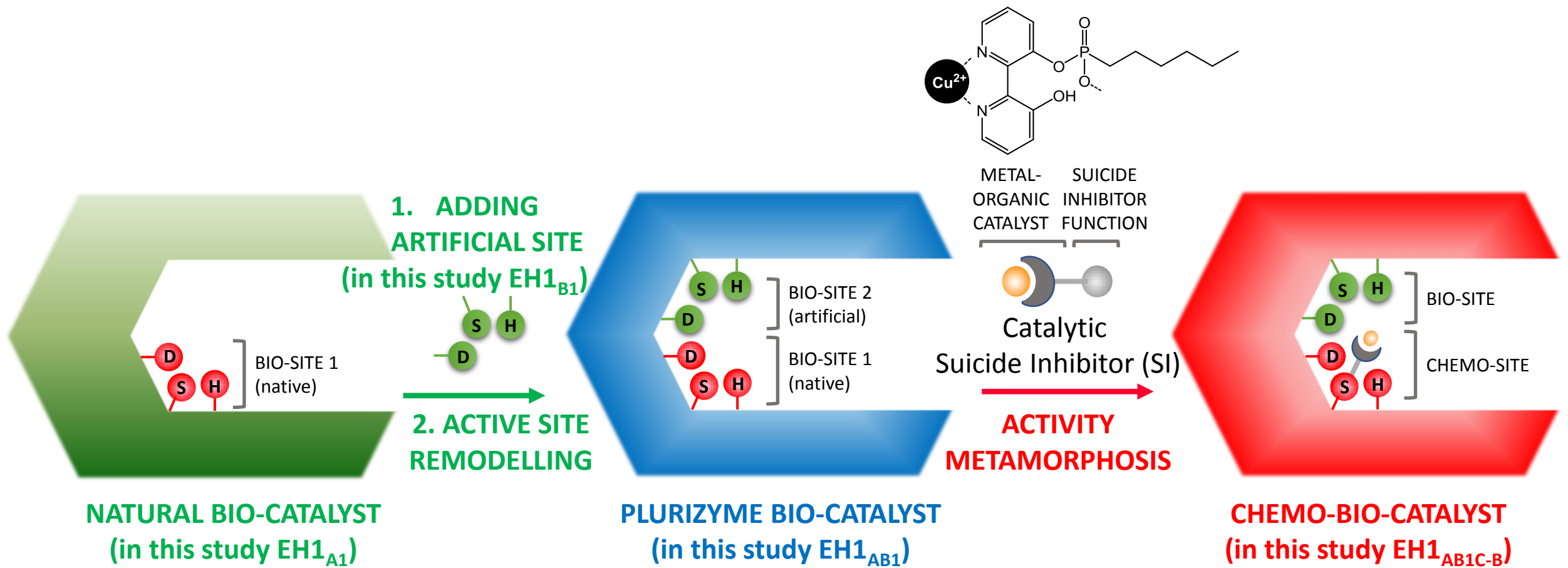
517 The authors declare no competing interests.

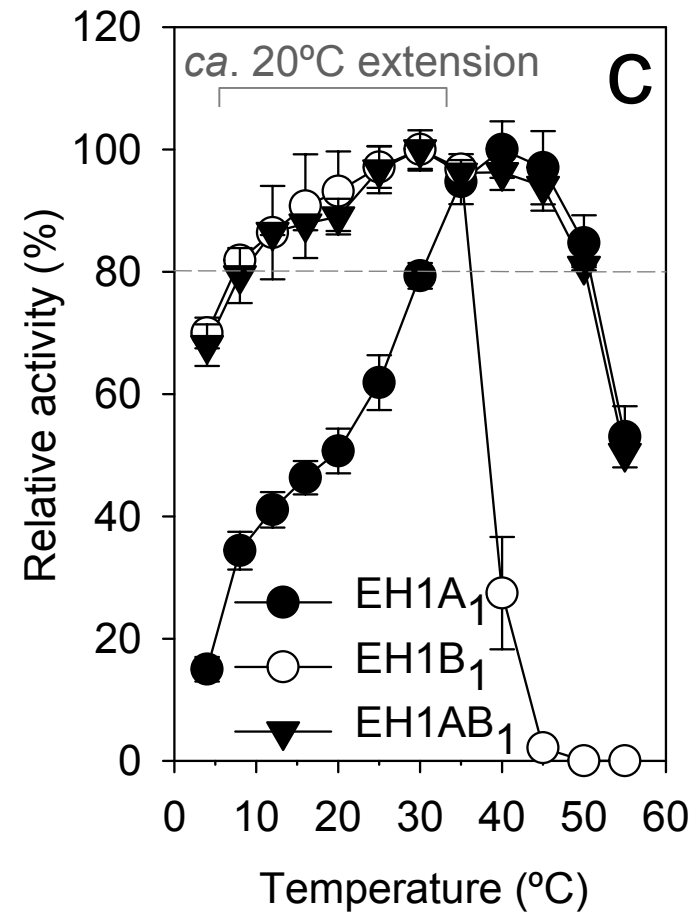
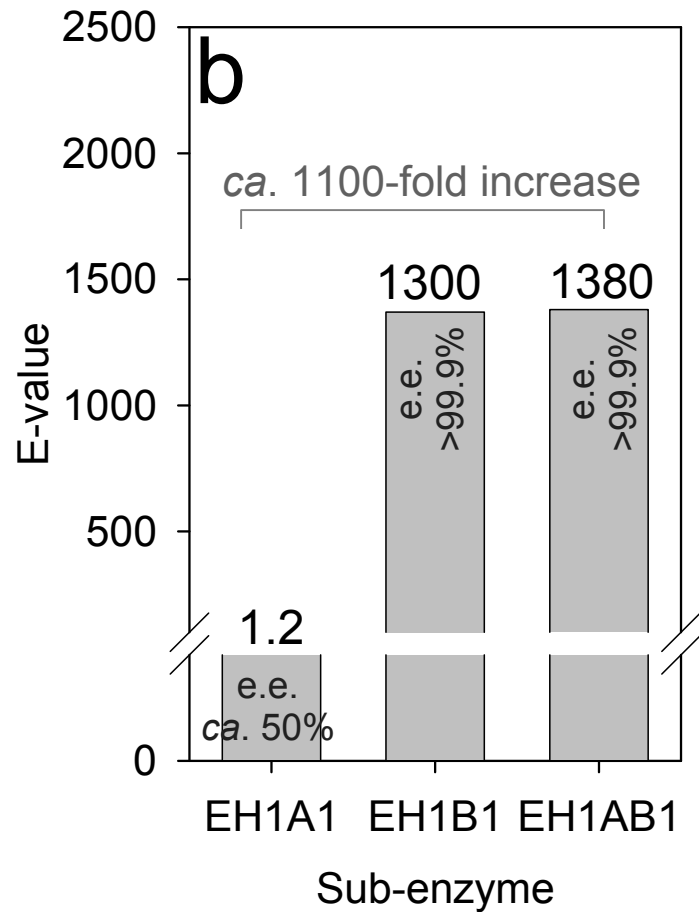
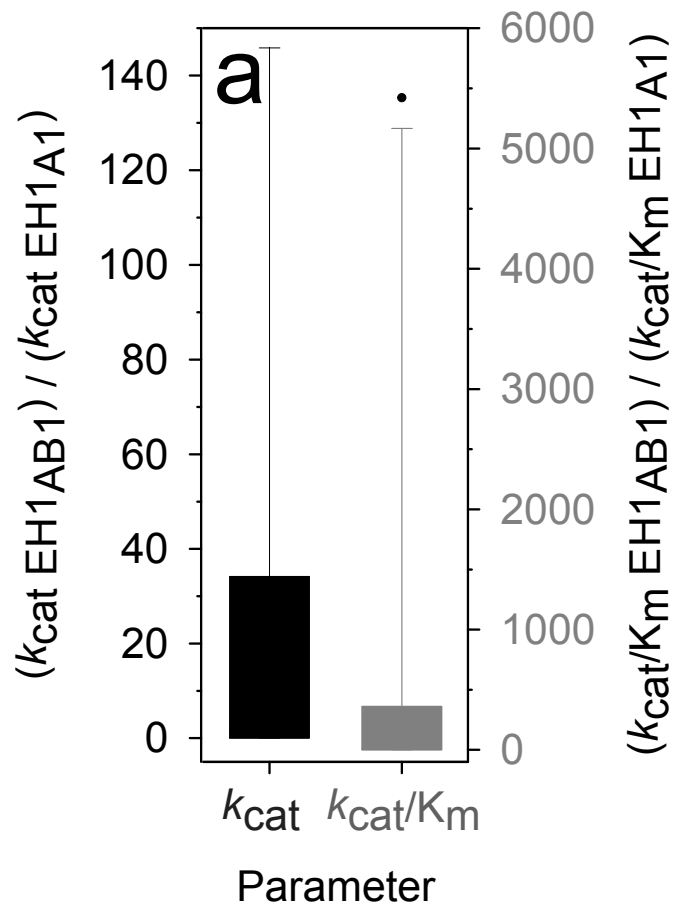
518

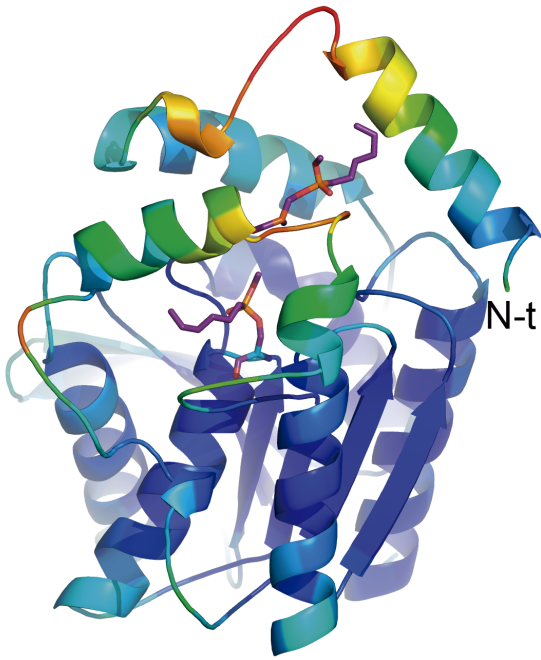
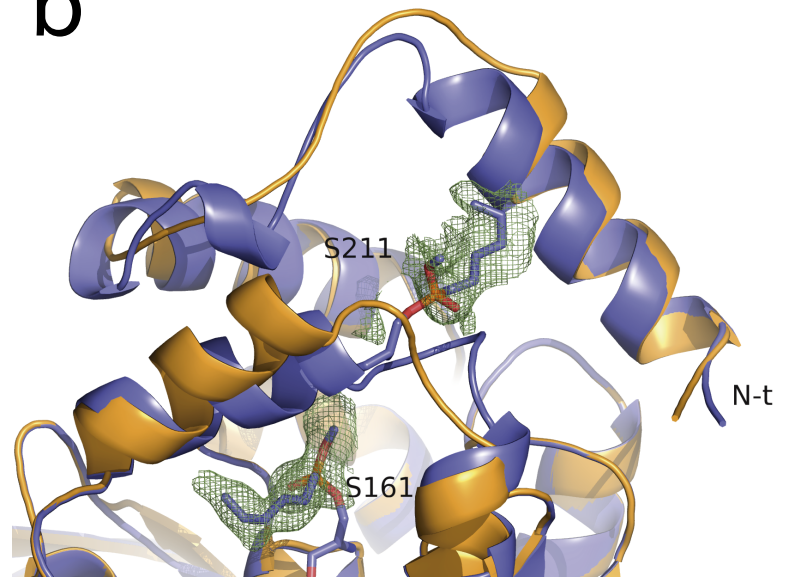
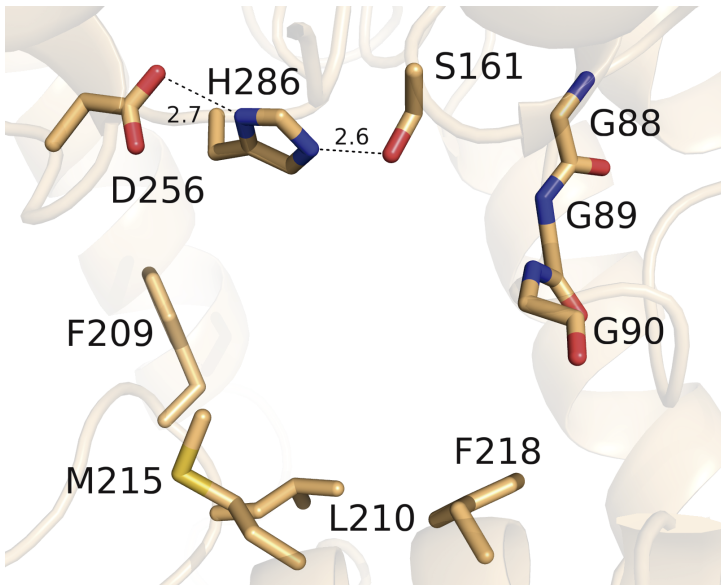
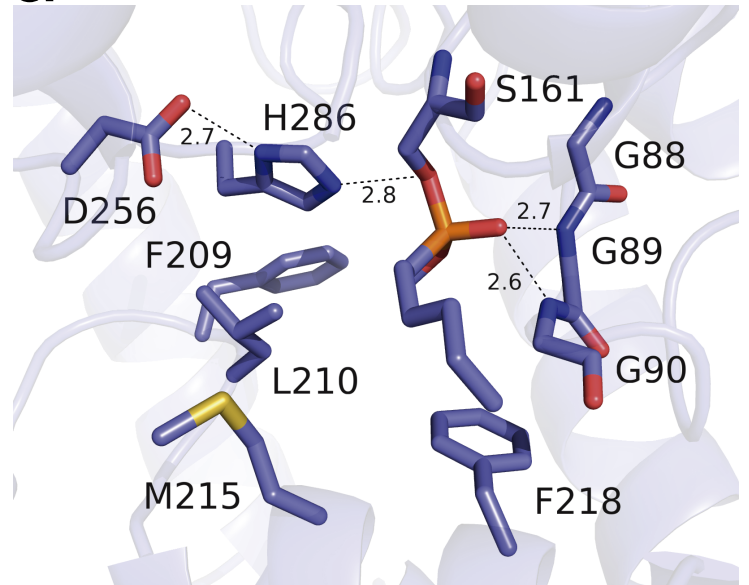
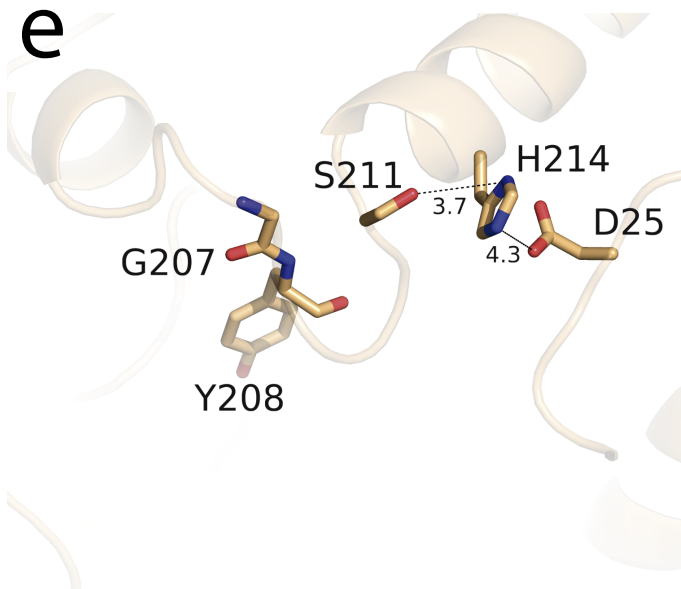
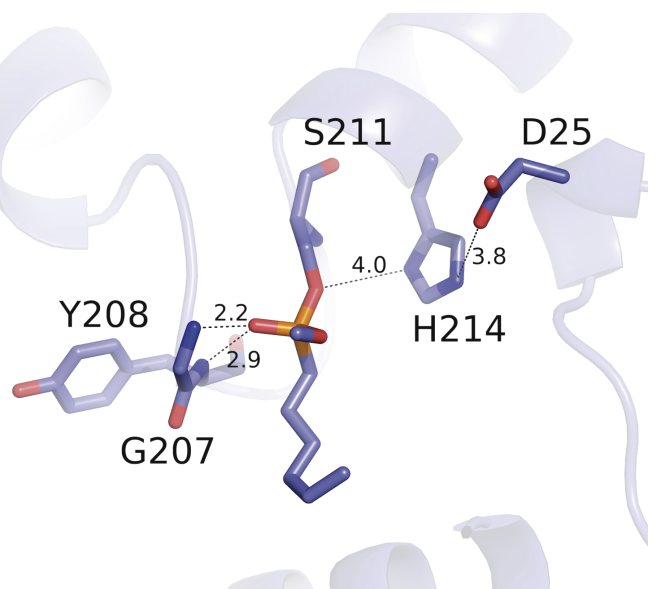
519 **Additional information**

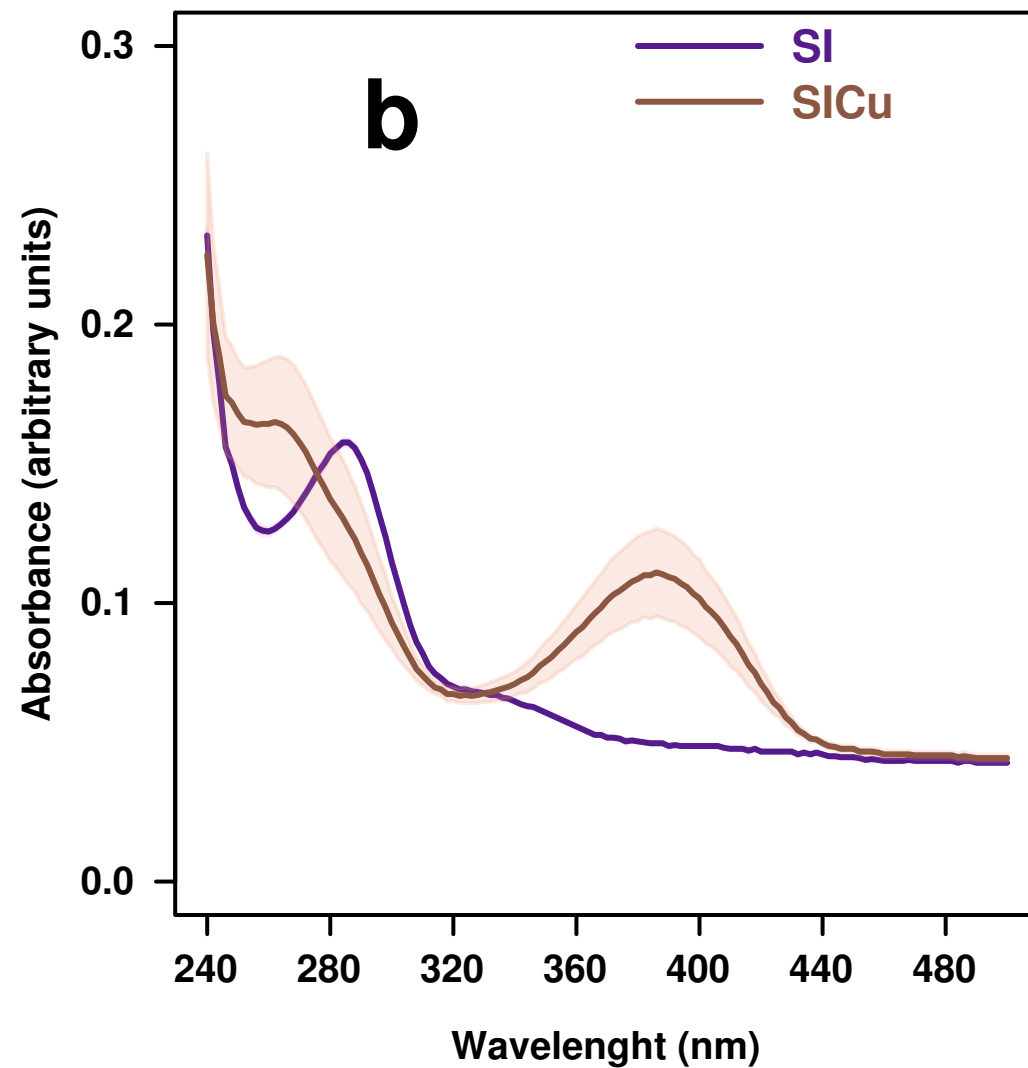
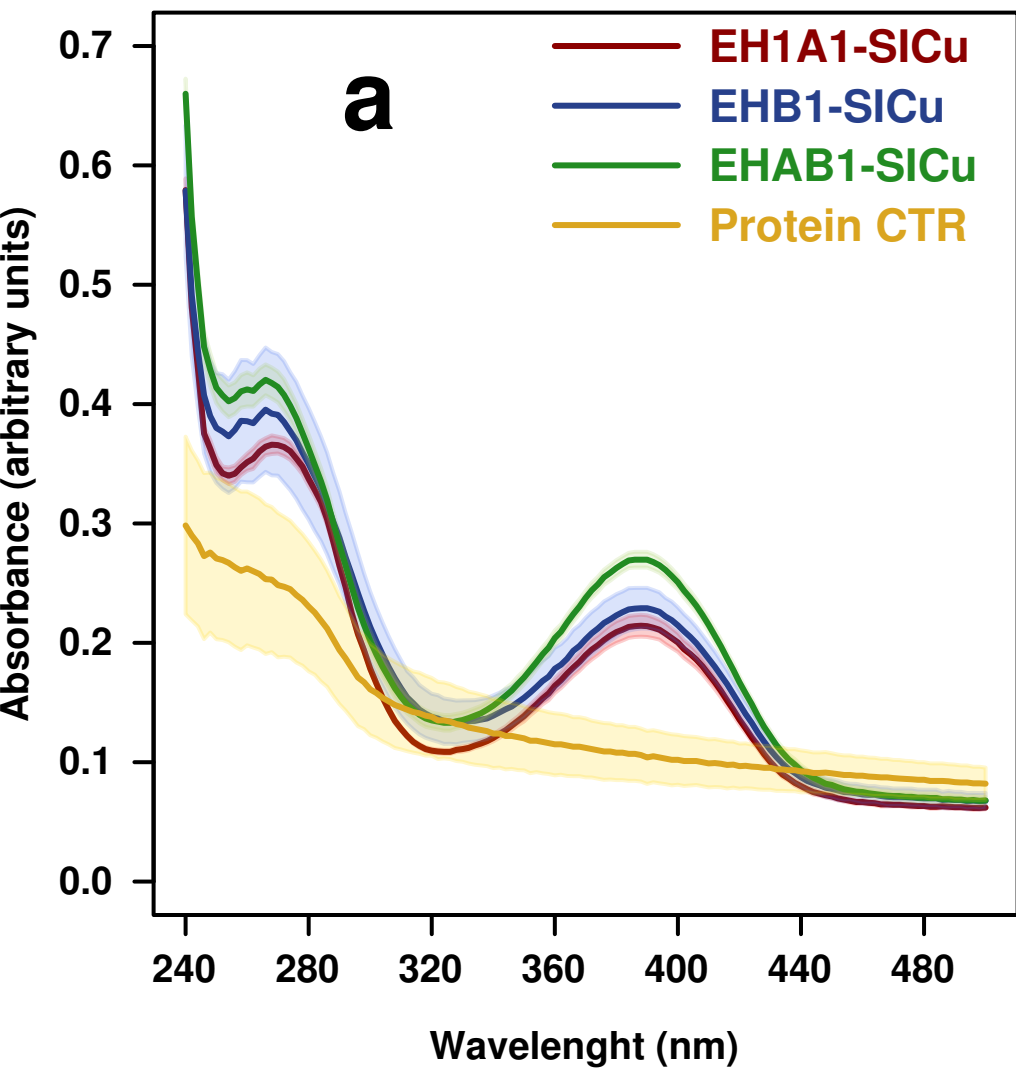
520 **Supplementary information** in available for this paper.

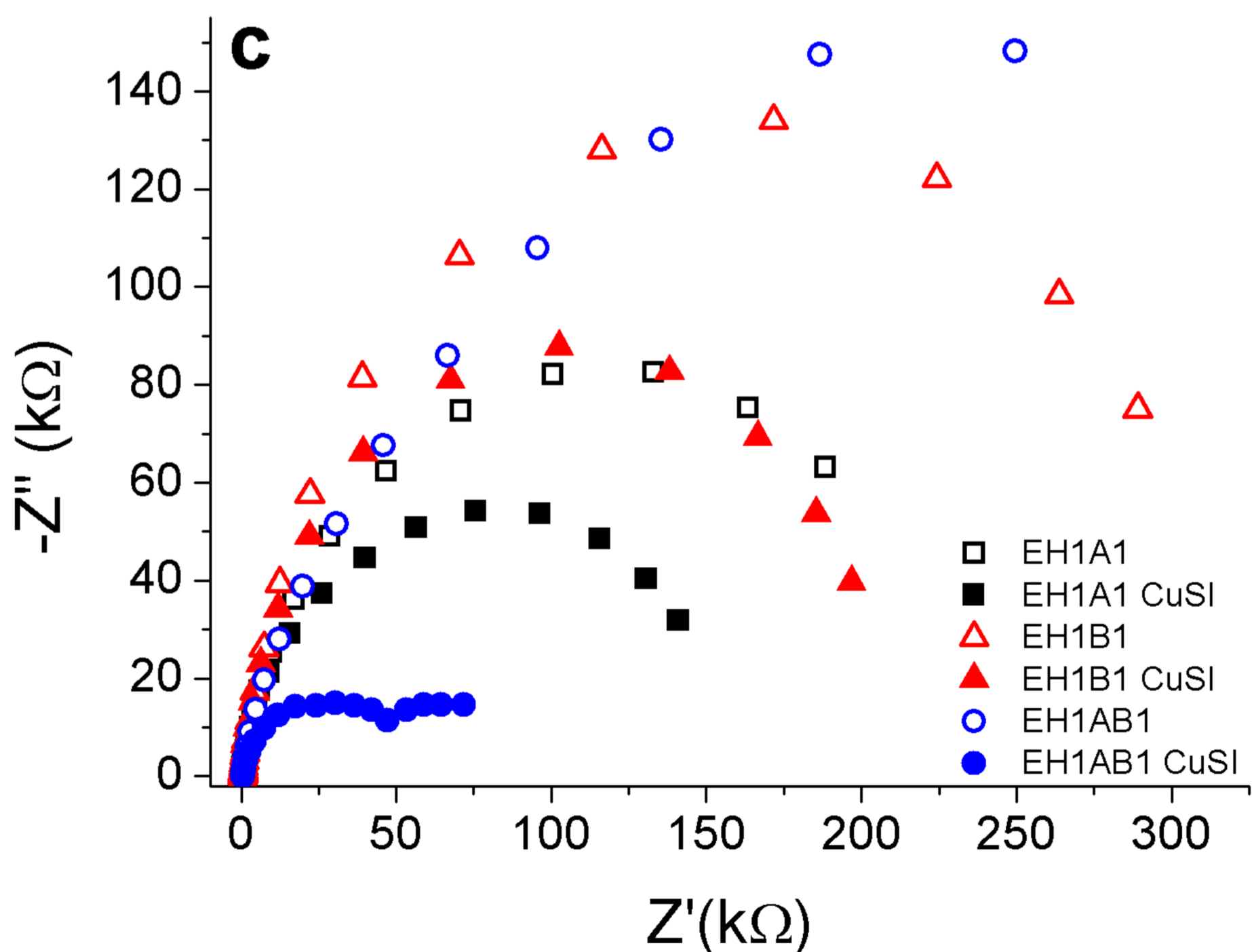
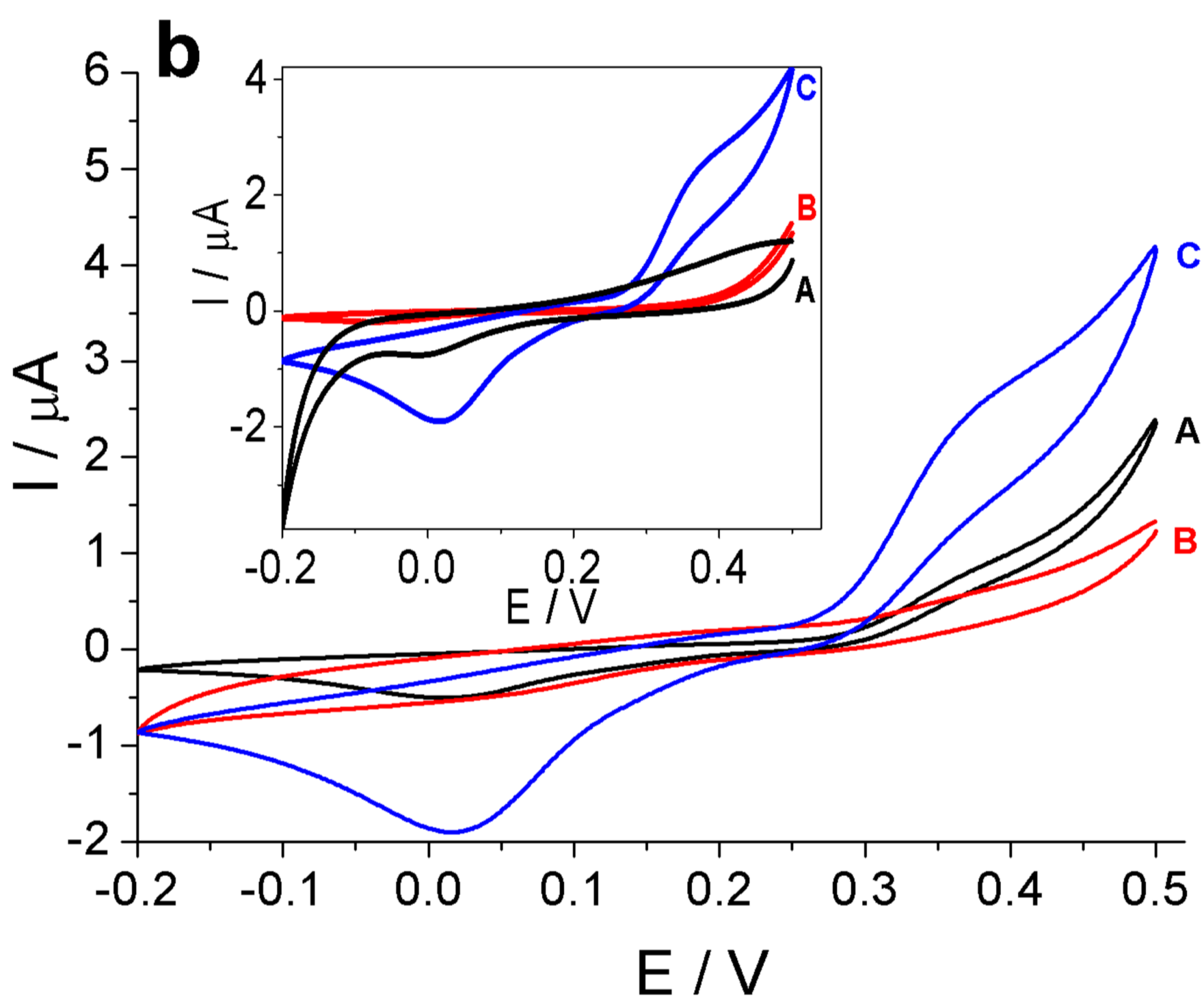
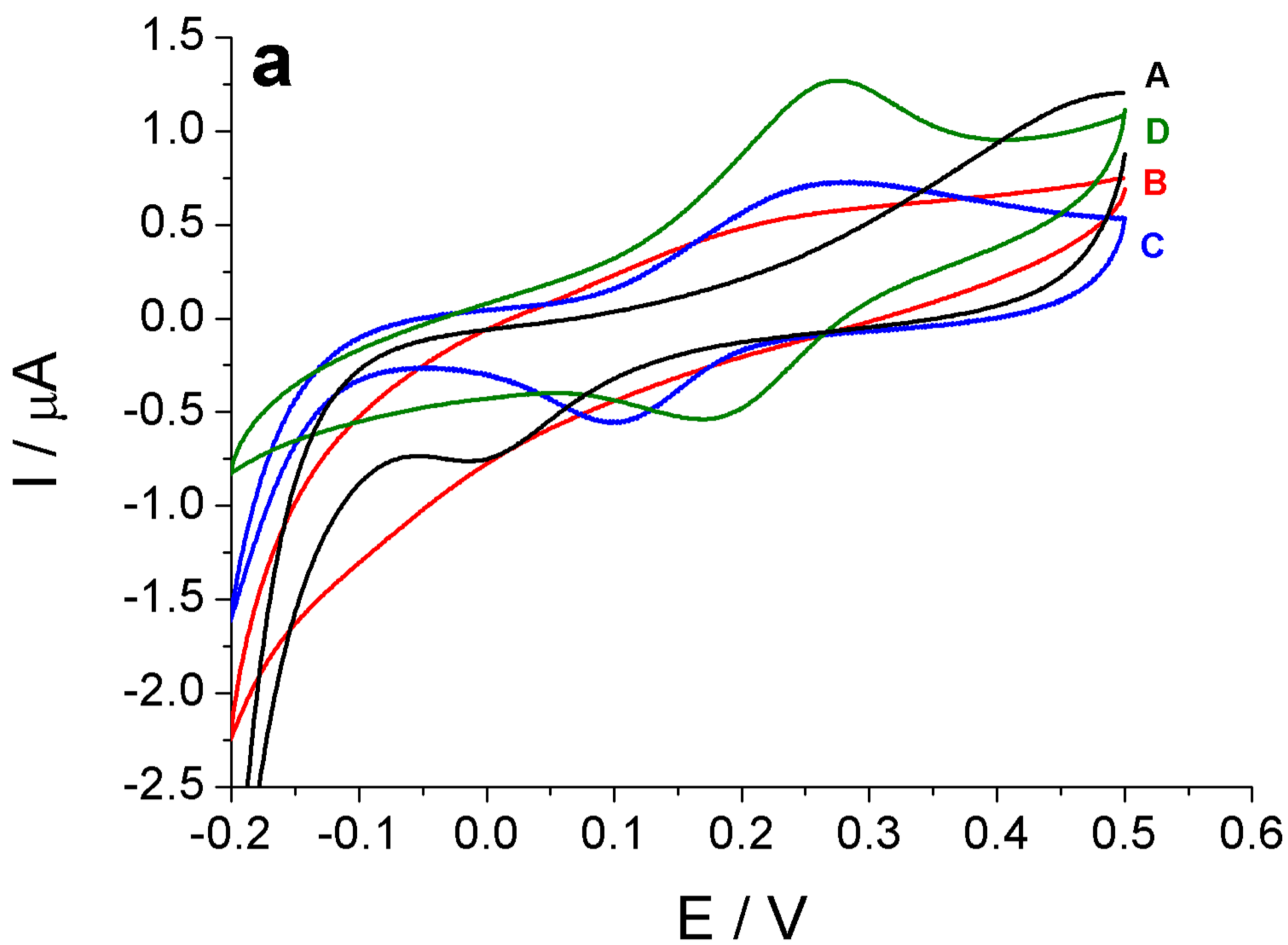
521 **Materials and correspondence** should be sent to M. F., V. G. or J. S-A.

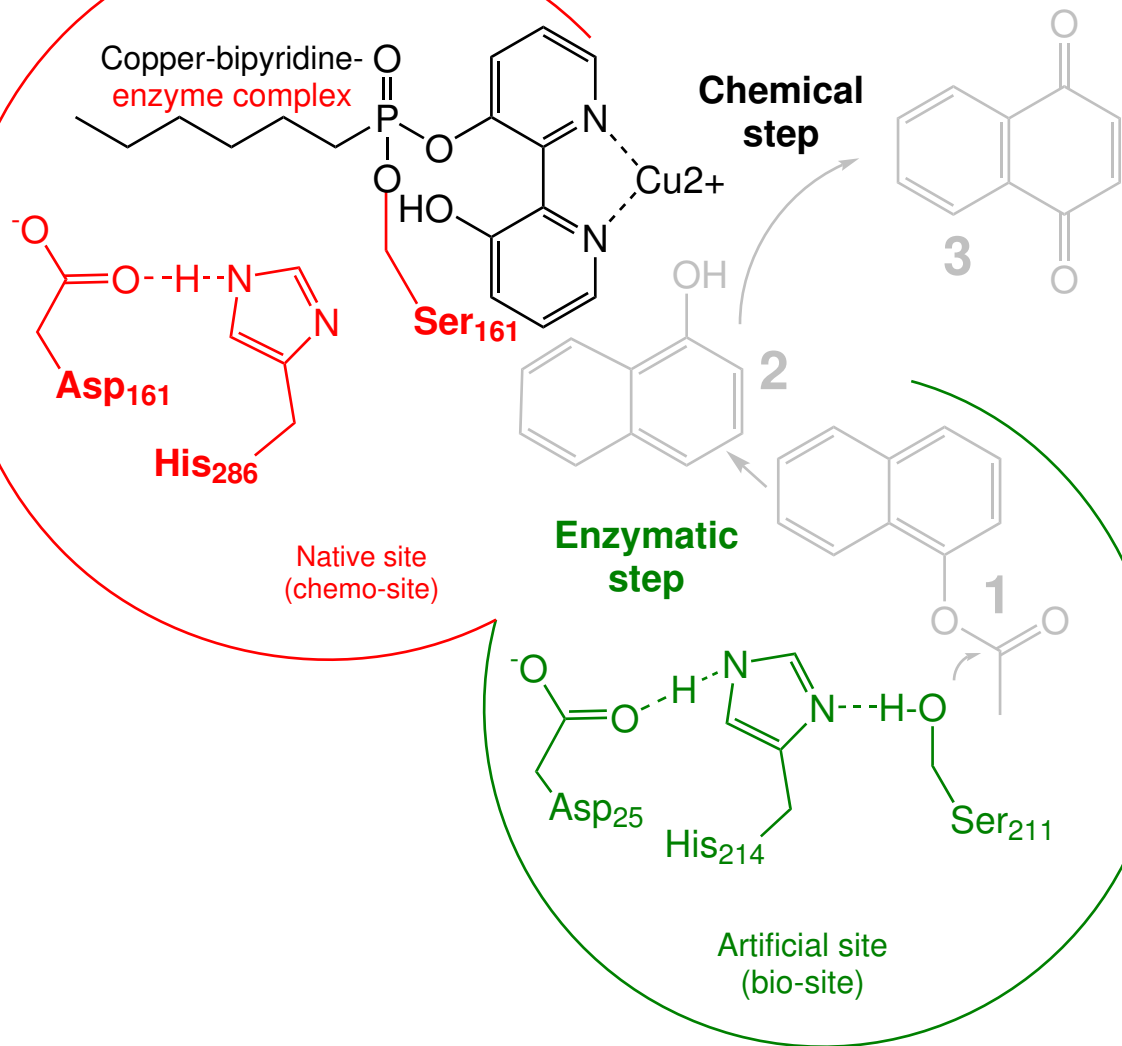
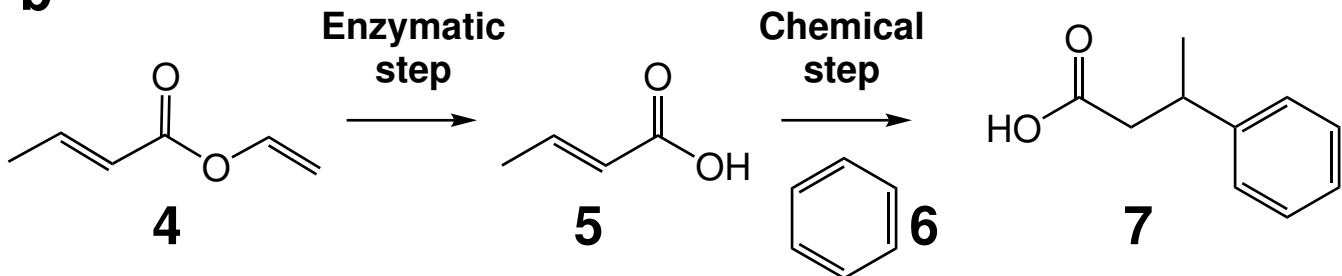


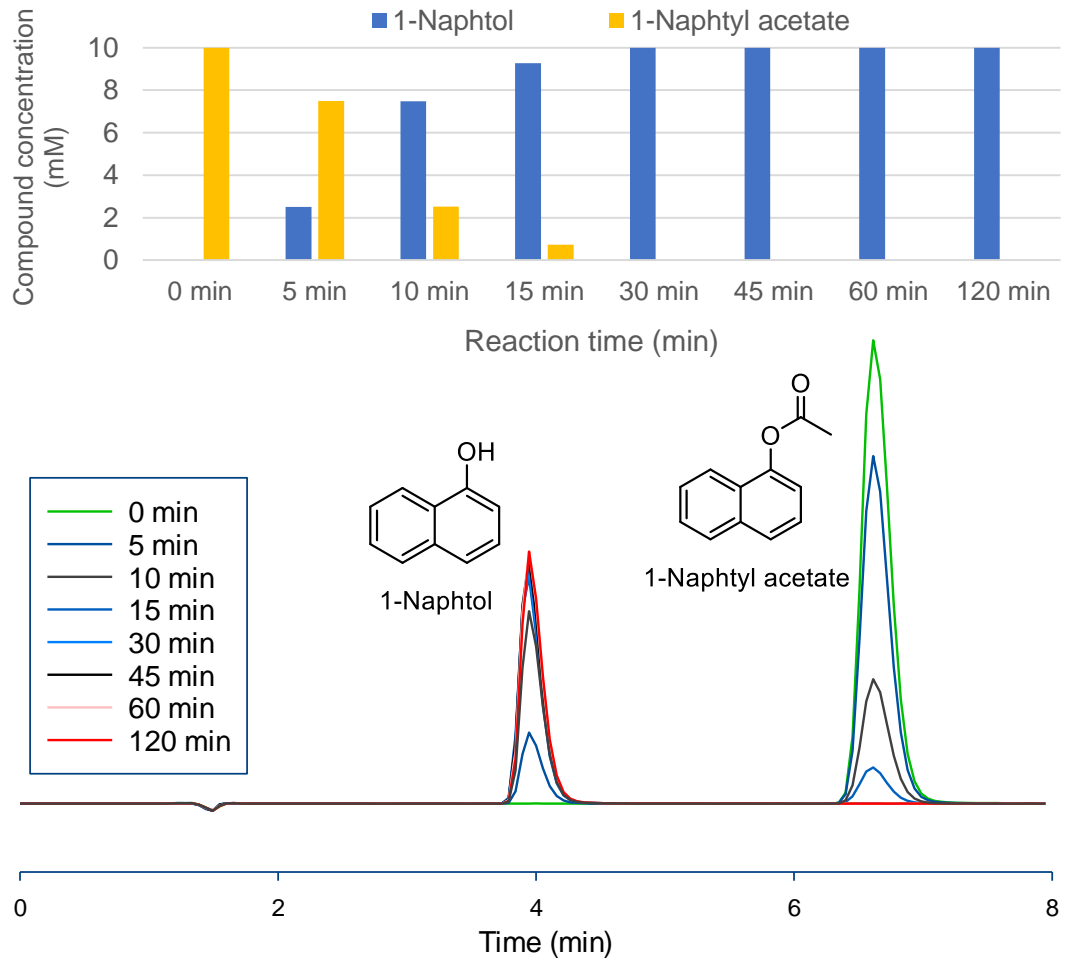
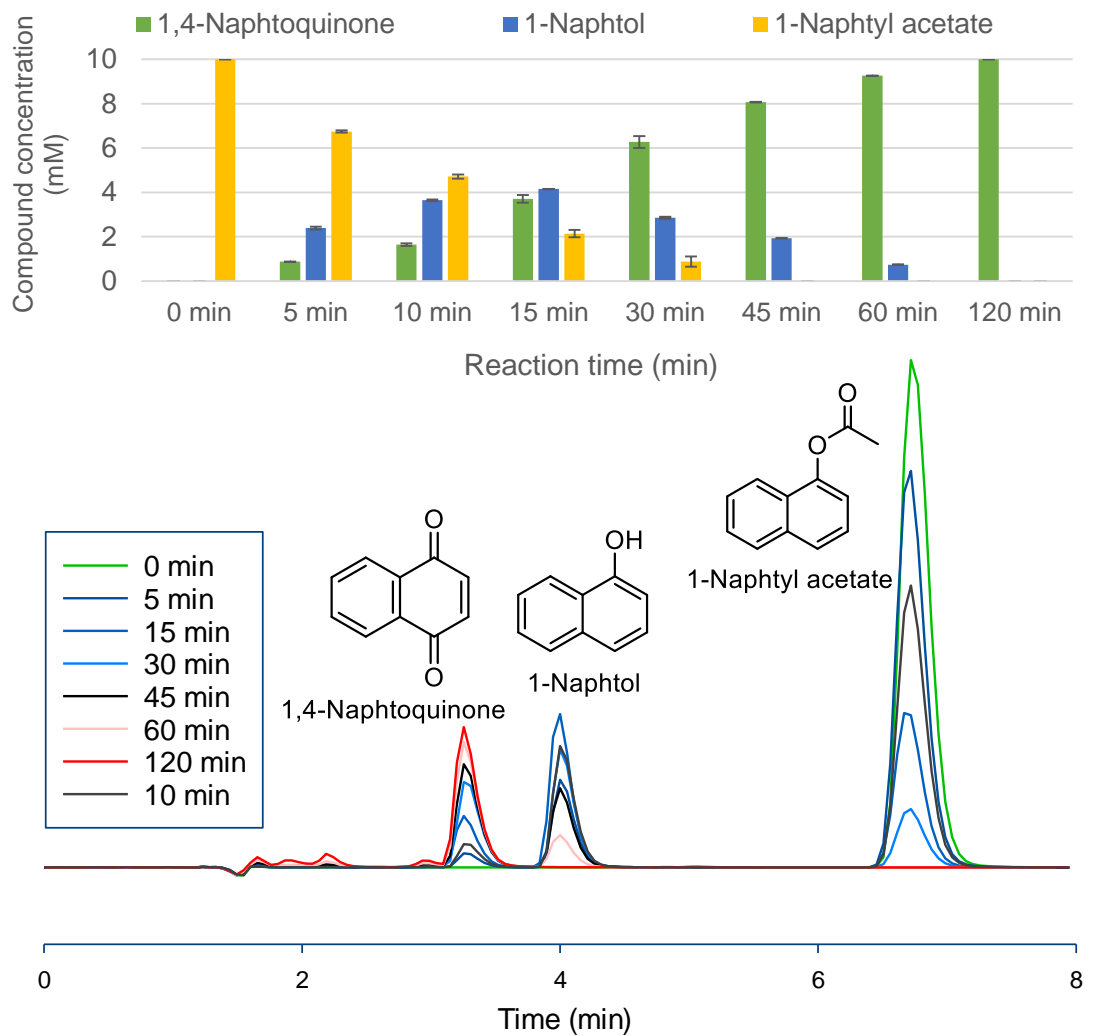


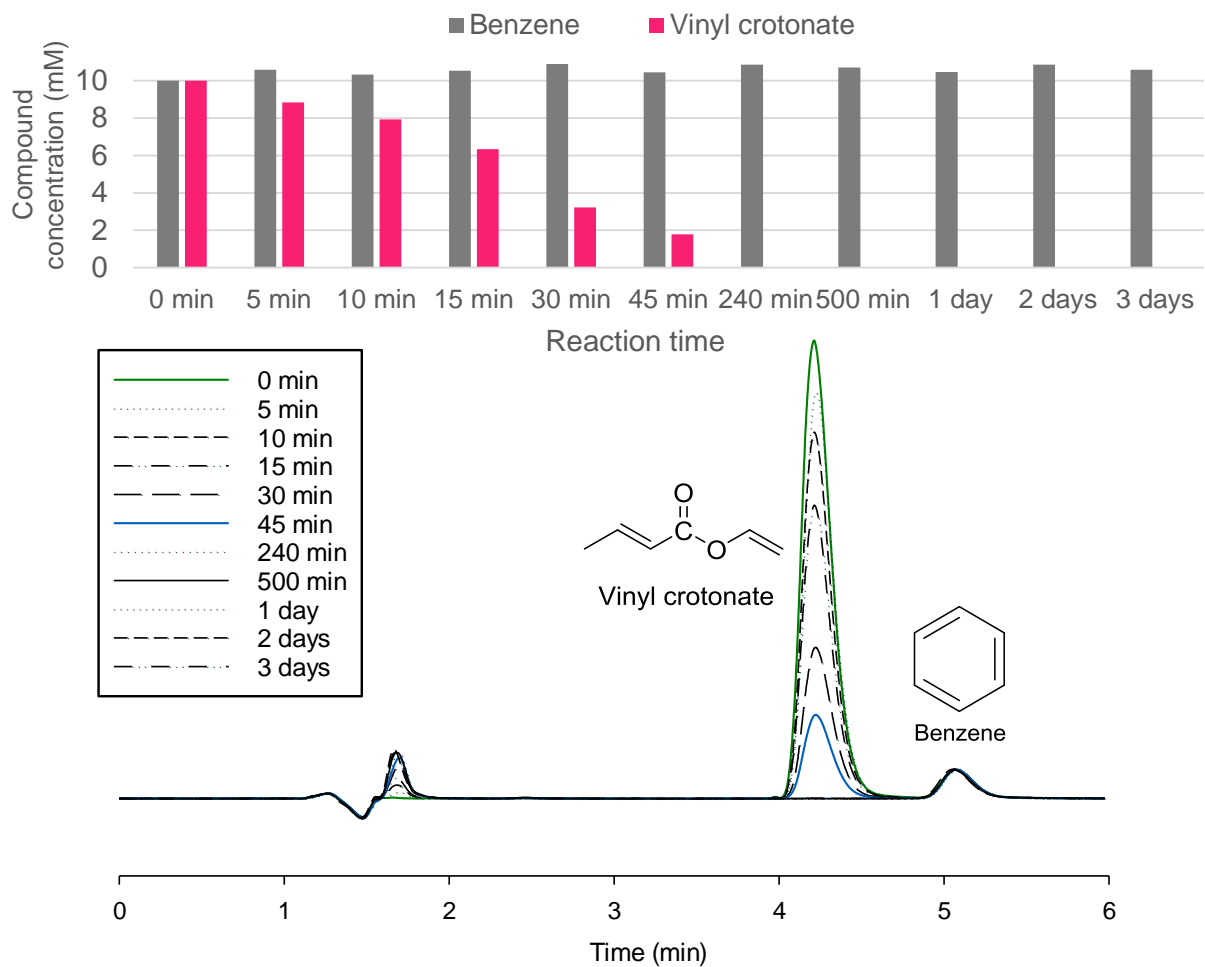
a**b****c****d****e****f**





a**b**

a**b**

a**b**